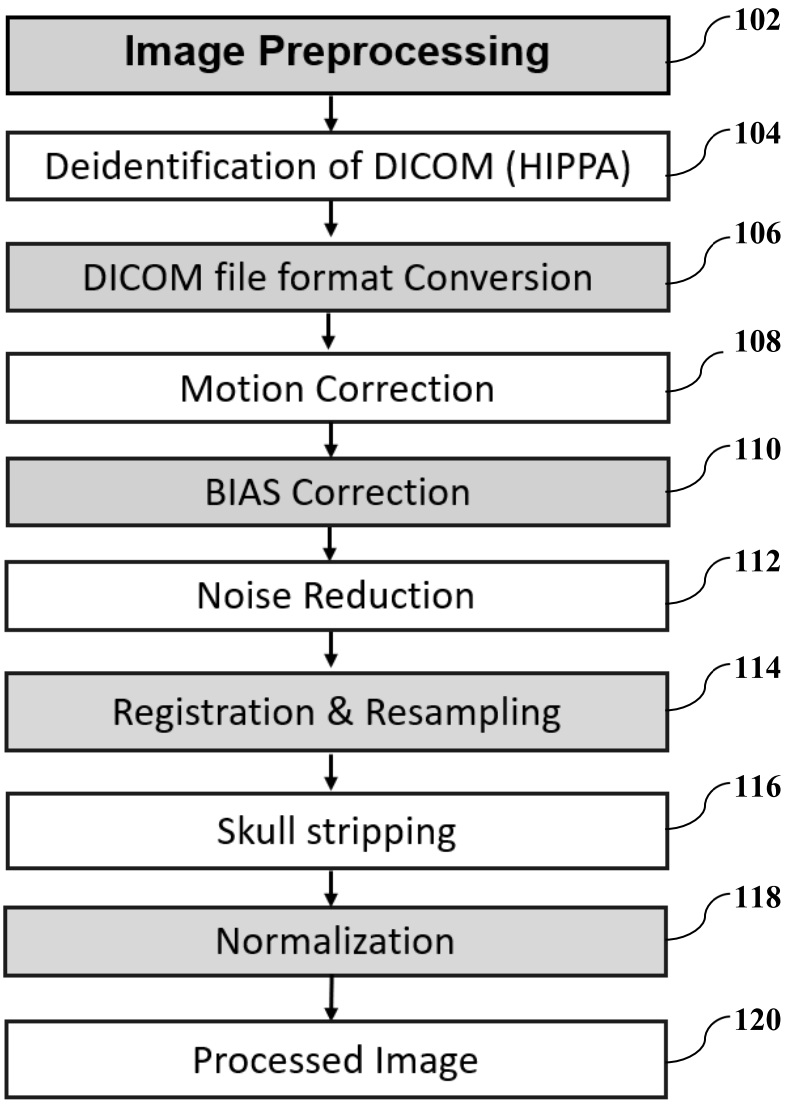


FIG. 1

Signature: -Sd-

Name: Dr Lipika Sahoo

Registration Number: IN/PA 2467

Agent for Applicant

This document is signed with the digital signature of patent agent Dr Lipika Sahoo Registration Number: IN/PA 2467

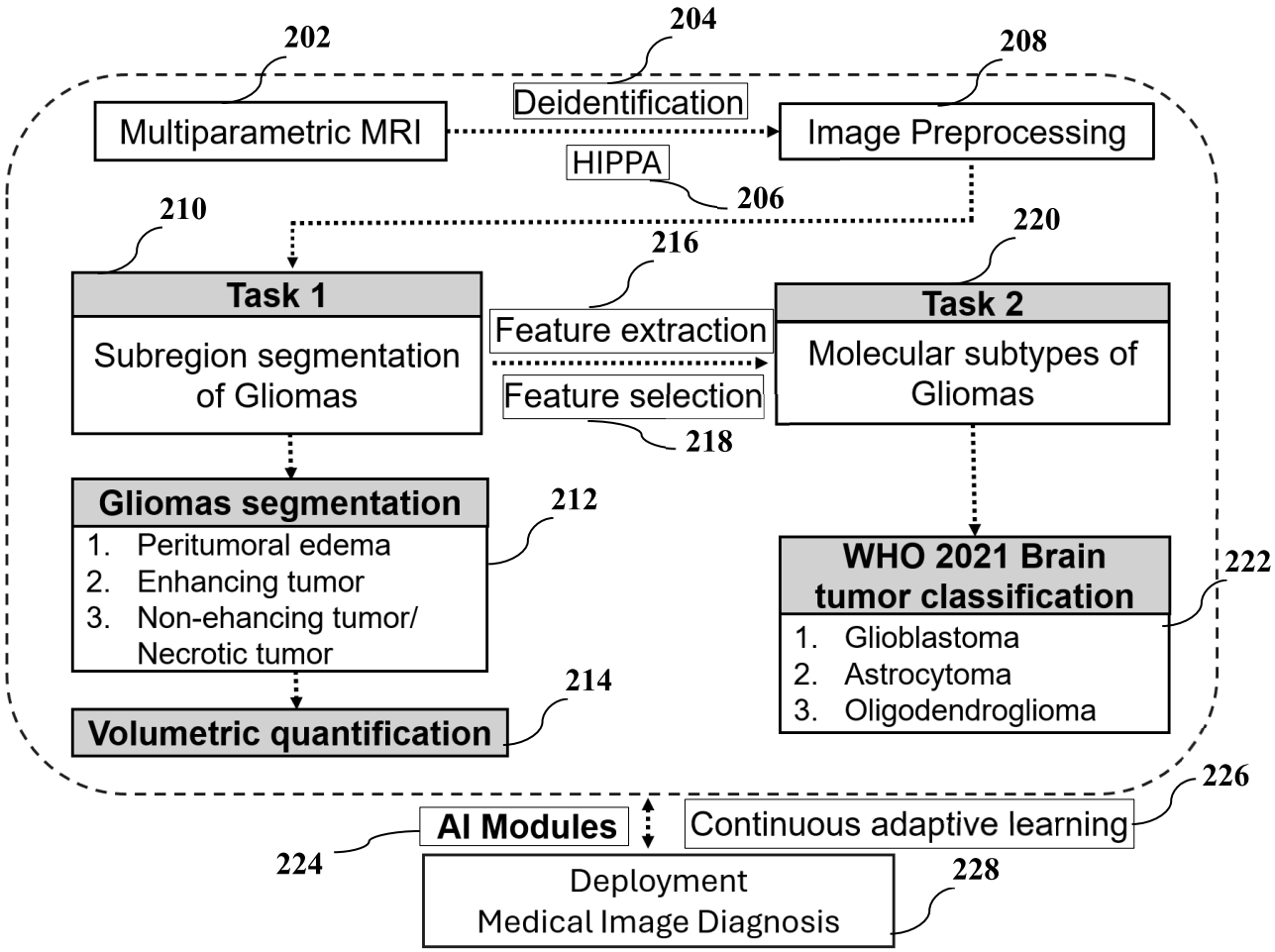


FIG. 2

Signature: -Sd-

Name: Dr Lipika Sahoo

Registration Number: IN/PA 2467

Agent for Applicant

This document is signed with the digital signature of patent agent Dr Lipika Sahoo Registration Number: IN/PA 2467

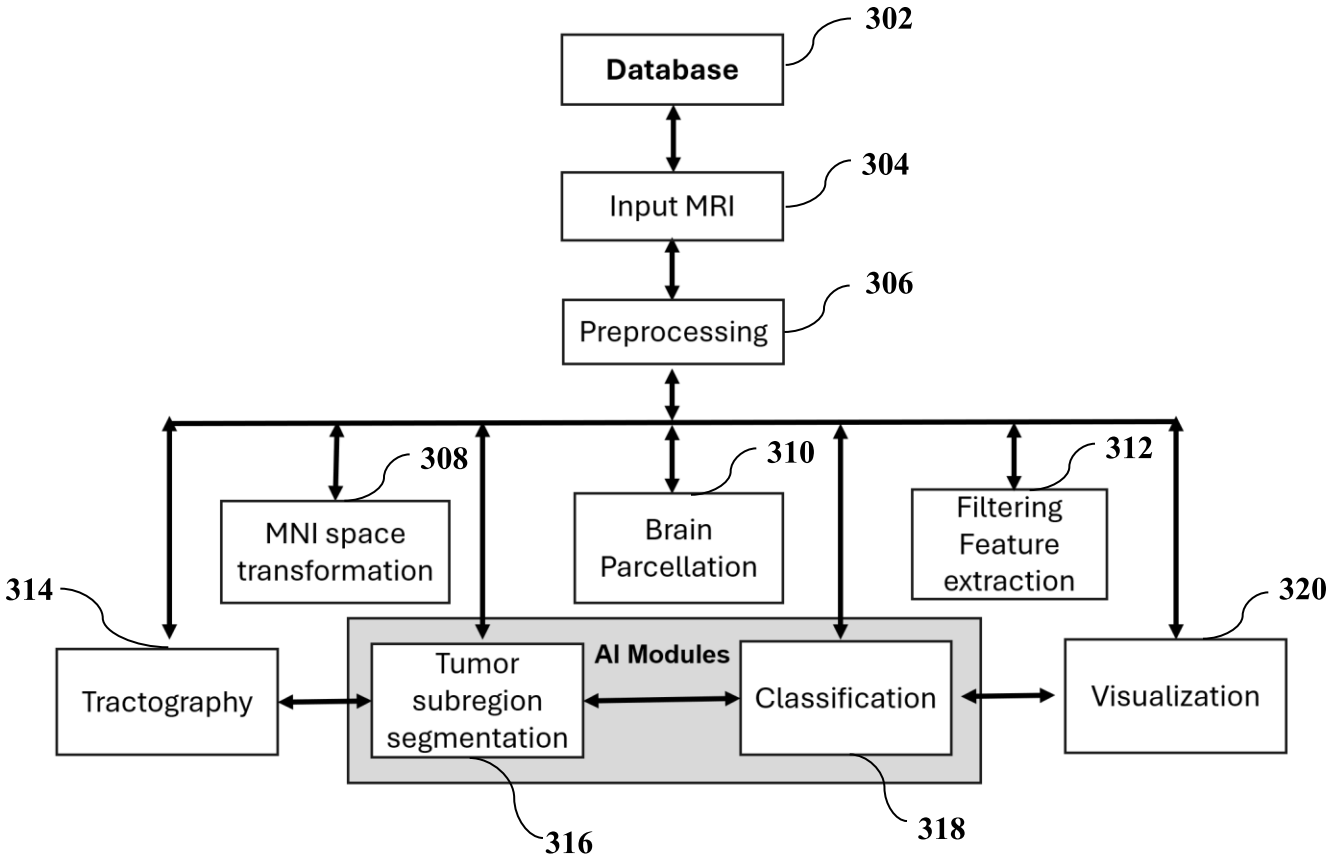


FIG. 3

Signature: -Sd-
Name: Dr Lipika Sahoo
Registration Number: IN/PA 2467
Agent for Applicant

This document is signed with the digital signature of patent agent Dr Lipika Sahoo Registration Number: IN/PA 2467

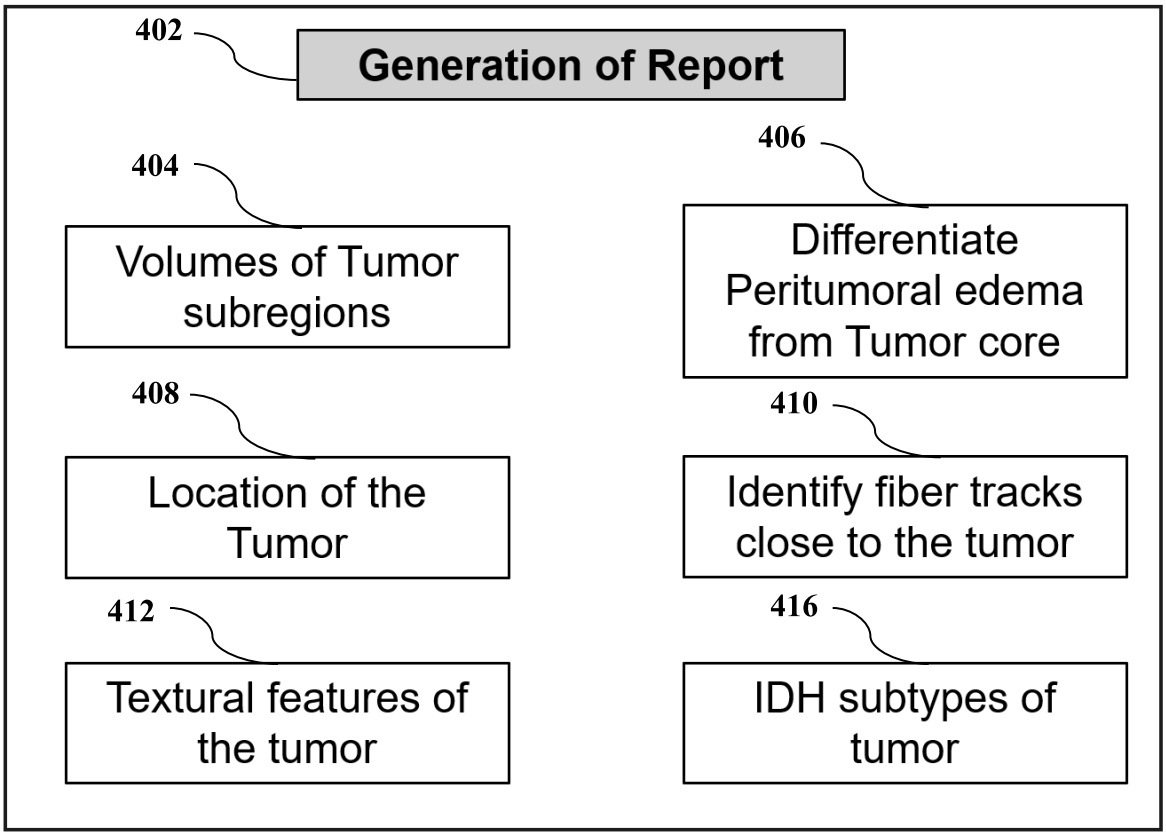


FIG. 4

Signature: -Sd-

Name: Dr Lipika Sahoo

Registration Number: IN/PA 2467

Agent for Applicant

This document is signed with the digital signature of patent agent Dr Lipika Sahoo Registration Number: IN/PA 2467

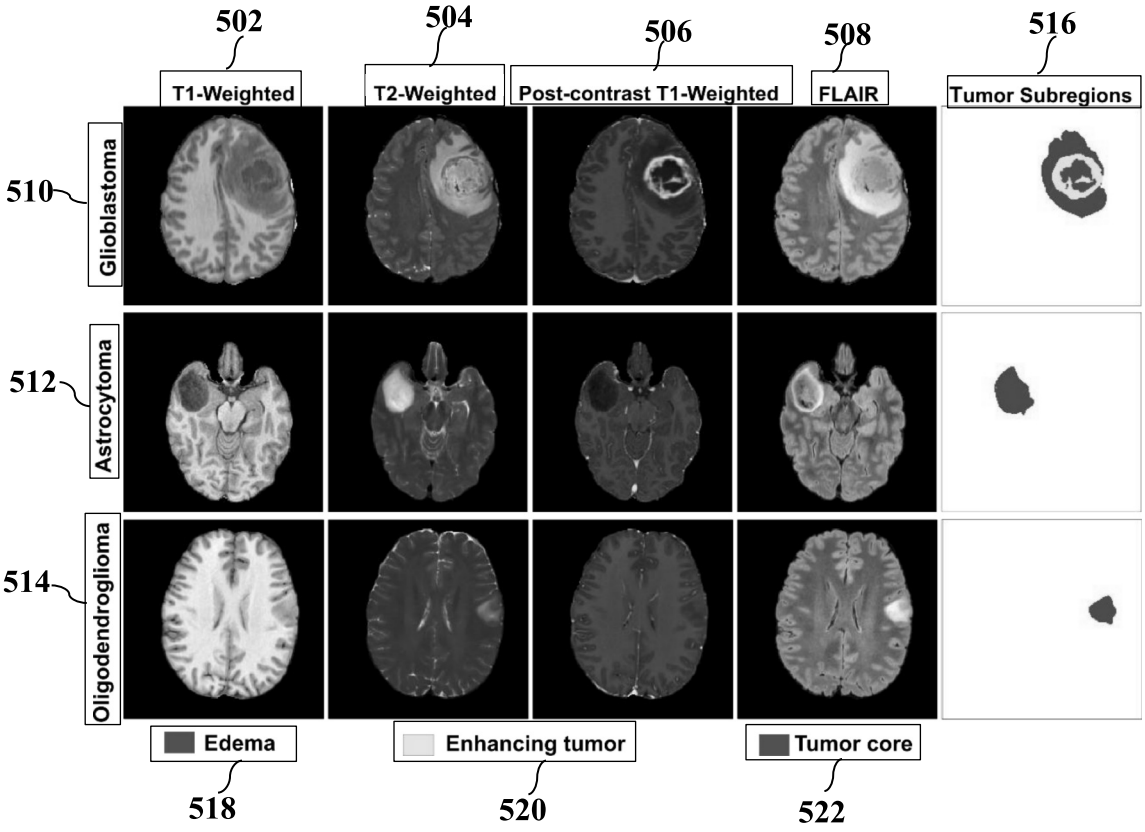


FIG. 5

Signature: -Sd-

Name: Dr Lipika Sahoo

Registration Number: IN/PA 2467

Agent for Applicant

This document is signed with the digital signature of patent agent Dr Lipika Sahoo Registration Number: IN/PA 2467

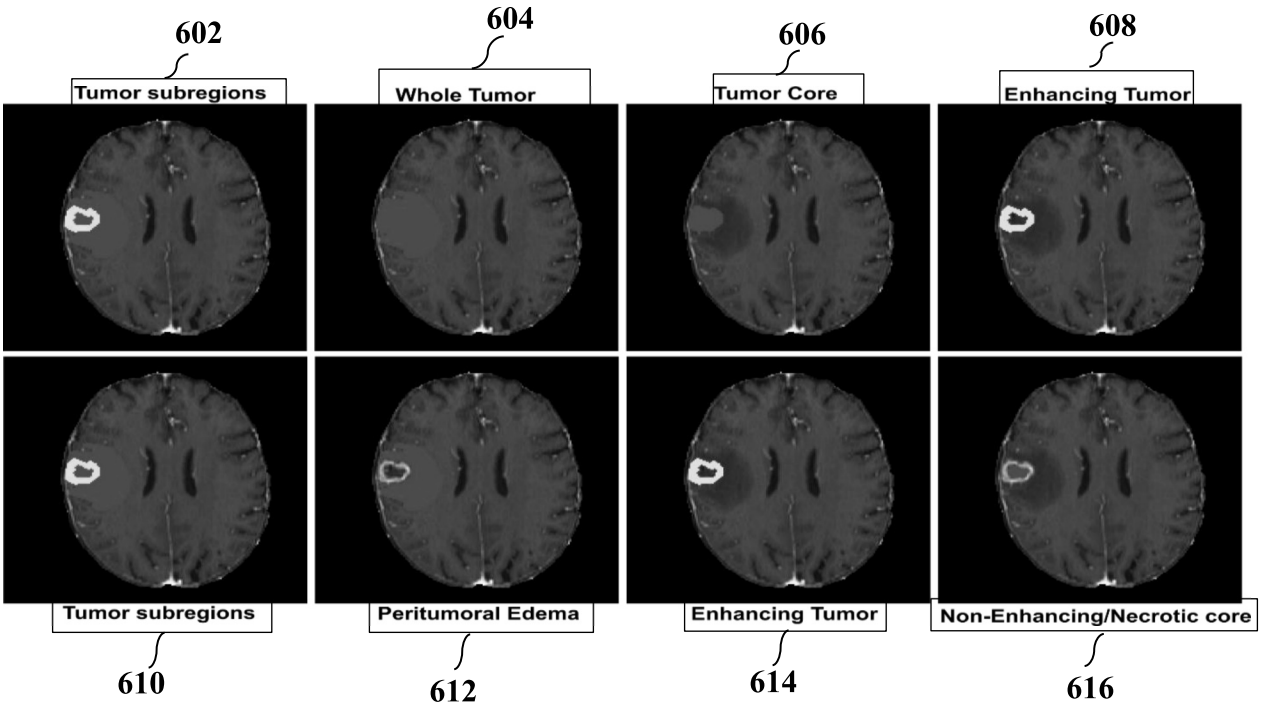


FIG. 6

Signature: -Sd-
Name: Dr Lipika Sahoo
Registration Number: IN/PA 2467
Agent for Applicant

This document is signed with the digital signature of patent agent Dr Lipika Sahoo Registration Number: IN/PA 2467

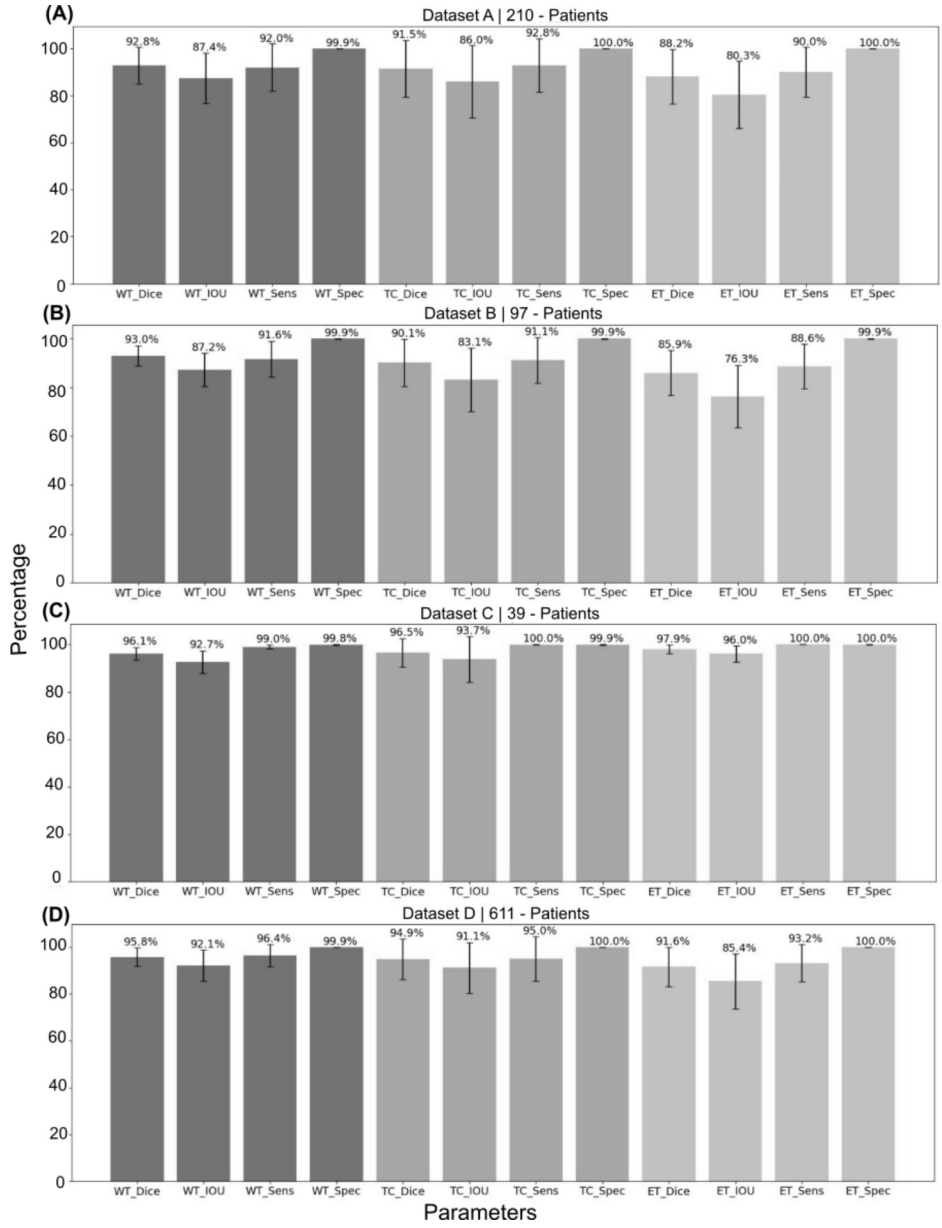


FIG. 7

Signature: -Sd-

Name: Dr Lipika Sahoo

Registration Number: IN/PA 2467

Agent for Applicant

This document is signed with the digital signature of patent agent Dr Lipika Sahoo Registration Number: IN/PA 2467

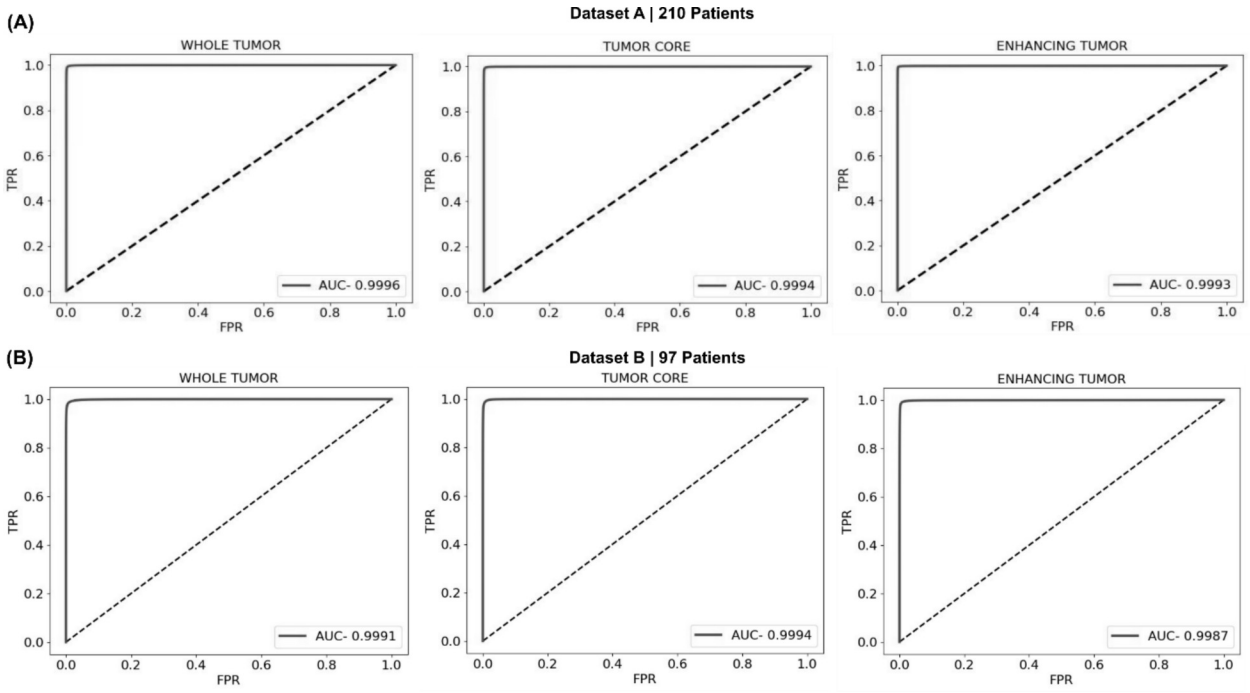


FIG. 8

Signature: -Sd-
Name: Dr Lipika Sahoo
Registration Number: IN/PA 2467
Agent for Applicant

This document is signed with the digital signature of patent agent Dr Lipika Sahoo Registration Number: IN/PA 2467

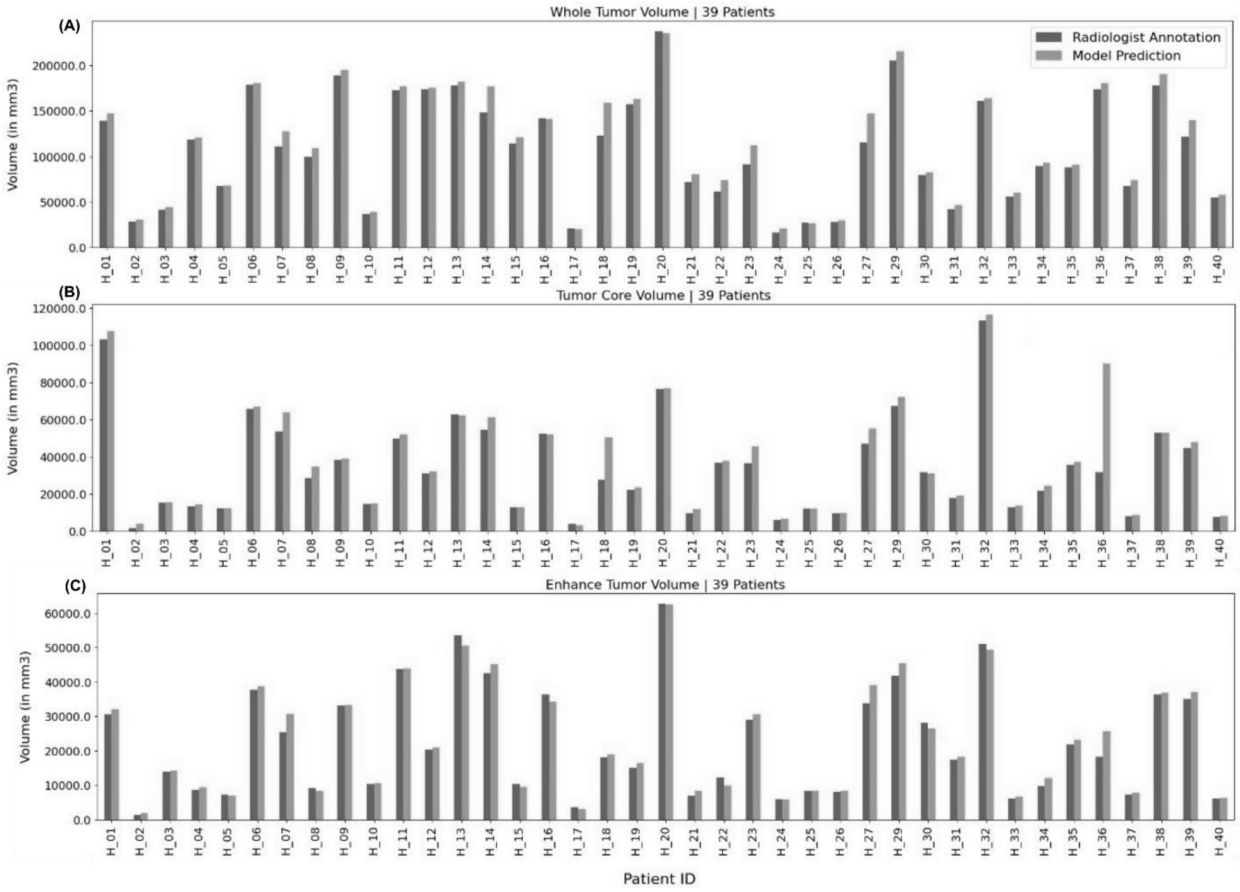


FIG. 9

Signature: -Sd-

Name: Dr Lipika Sahoo

Registration Number: IN/PA 2467

Agent for Applicant

This document is signed with the digital signature of patent agent Dr Lipika Sahoo Registration Number: IN/PA 2467

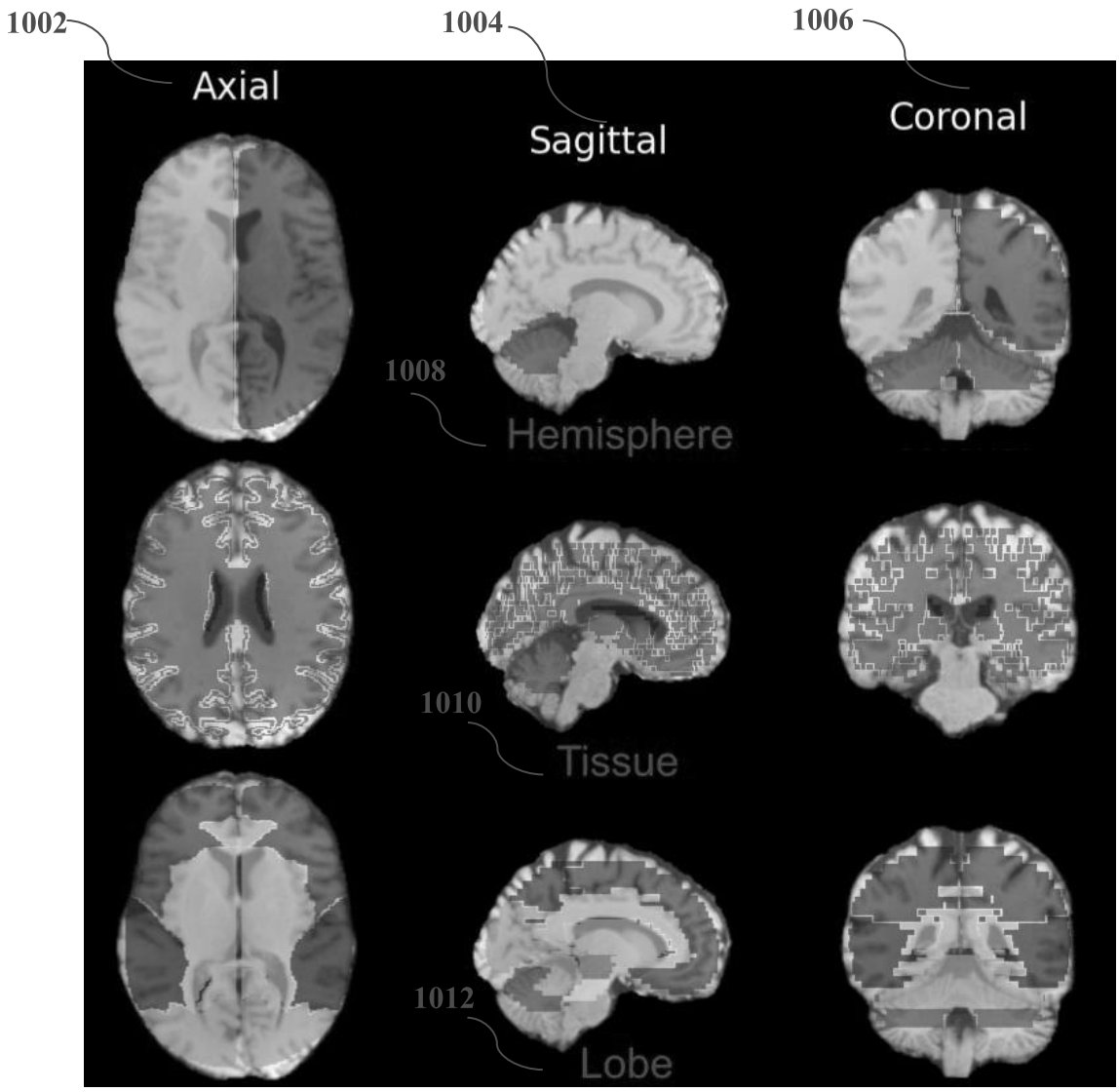


FIG. 10

Signature: -Sd-

Name: Dr Lipika Sahoo

Registration Number: IN/PA 2467

Agent for Applicant

This document is signed with the digital signature of patent agent Dr Lipika Sahoo Registration Number: IN/PA 246

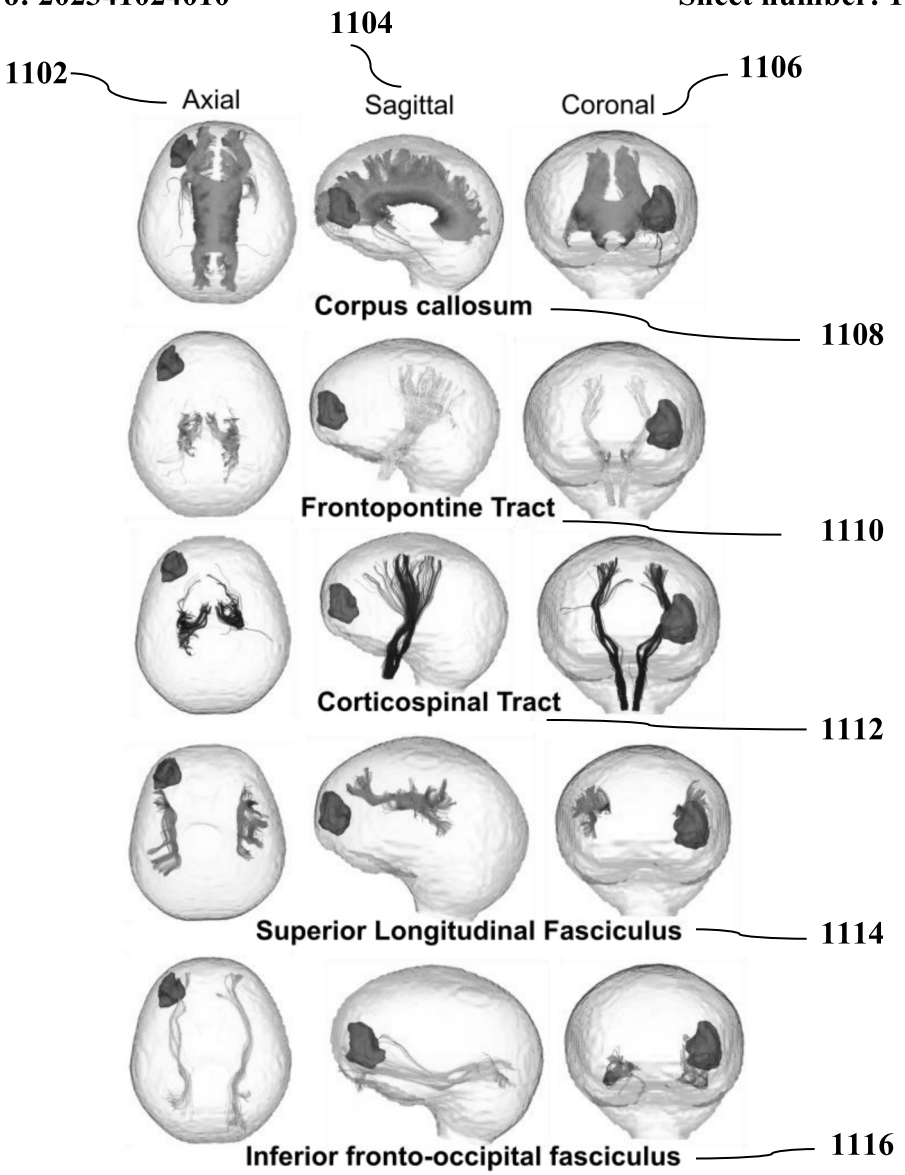


FIG. 11

Signature: -Sd-

Name: Dr Lipika Sahoo

Registration Number: IN/PA 2467

Agent for Applicant

This document is signed with the digital signature of patent agent Dr Lipika Sahoo Registration Number: IN/PA 246

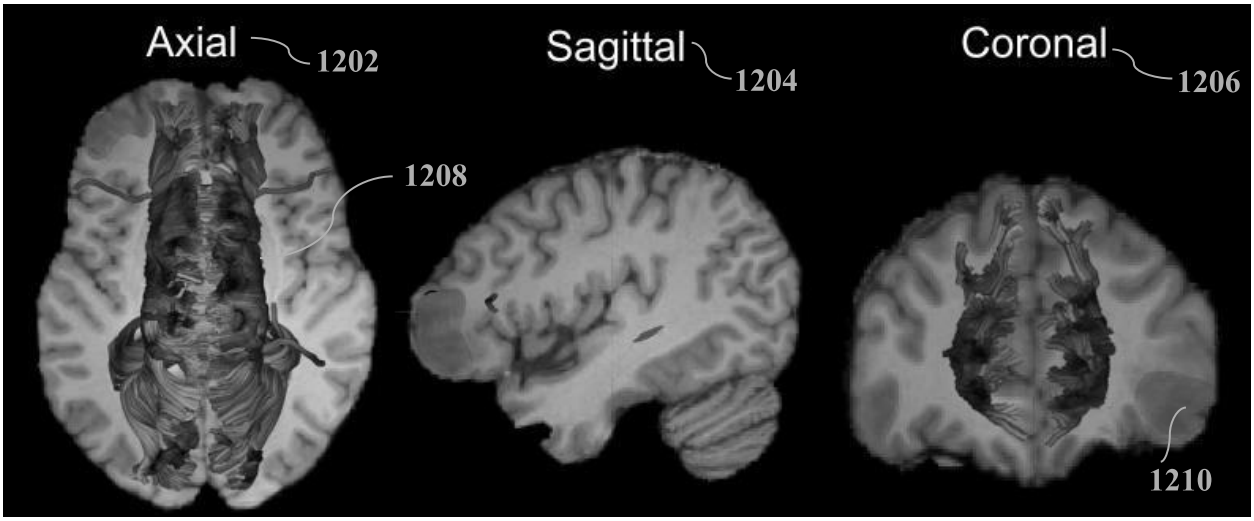


FIG. 12

Signature: -Sd-
Name: Dr Lipika Sahoo
Registration Number: IN/PA 2467
Agent for Applicant

This document is signed with the digital signature of patent agent Dr Lipika Sahoo Registration Number: IN/PA 246

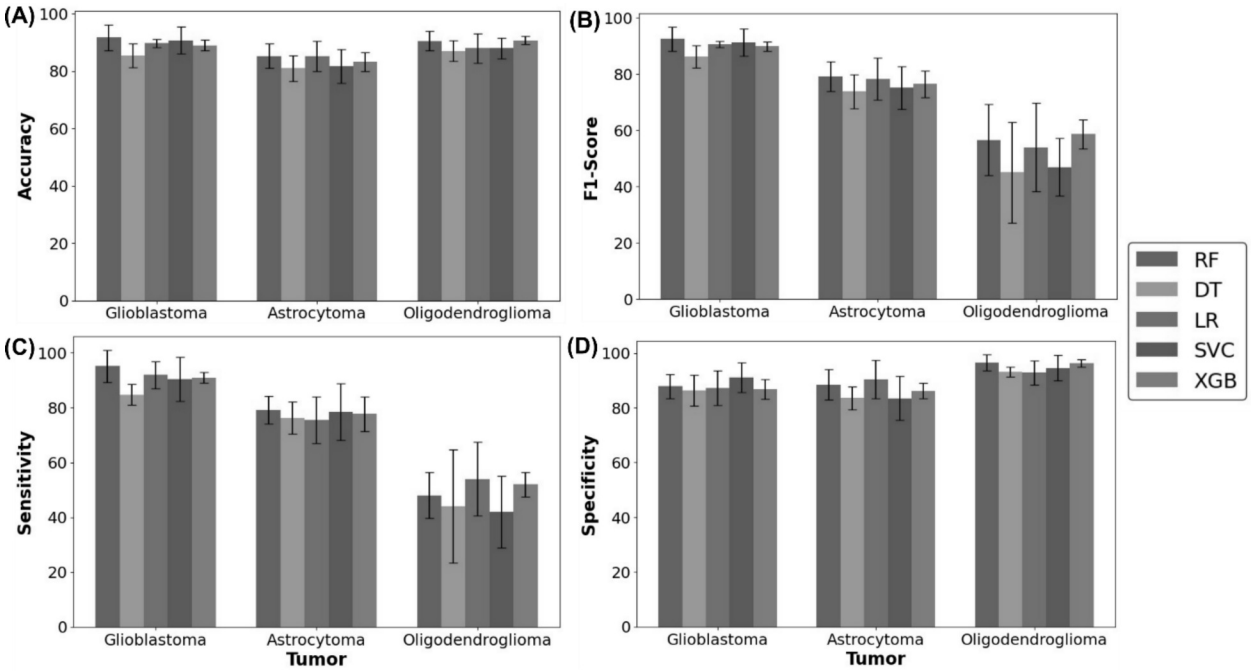


FIG. 13

Signature: -Sd-

Name: Dr Lipika Sahoo

Registration Number: IN/PA 2467

Agent for Applicant

This document is signed with the digital signature of patent agent Dr Lipika Sahoo Registration Number: IN/PA 2467

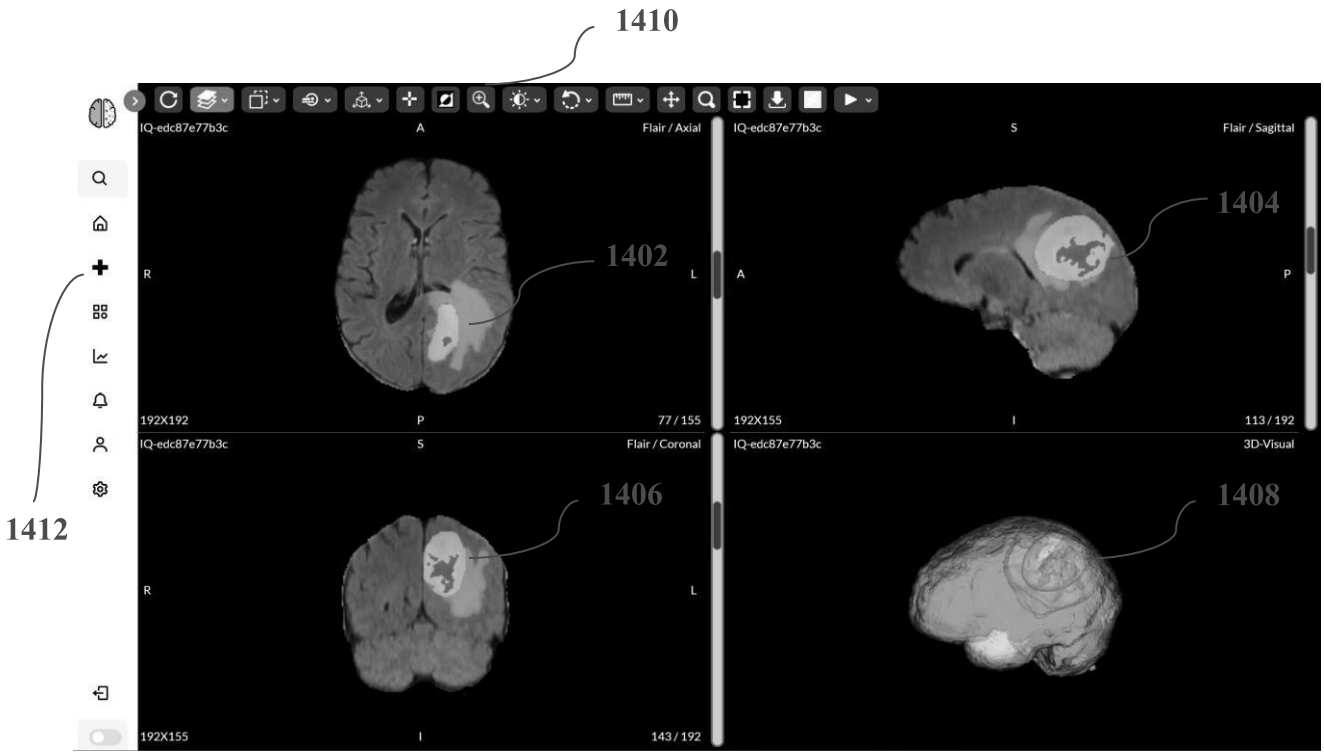


FIG. 14

Signature: -Sd-

Name: Dr Lipika Sahoo

Registration Number: IN/PA 2467

Agent for Applicant

This document is signed with the digital signature of patent agent Dr Lipika Sahoo Registration Number: IN/PA 2467

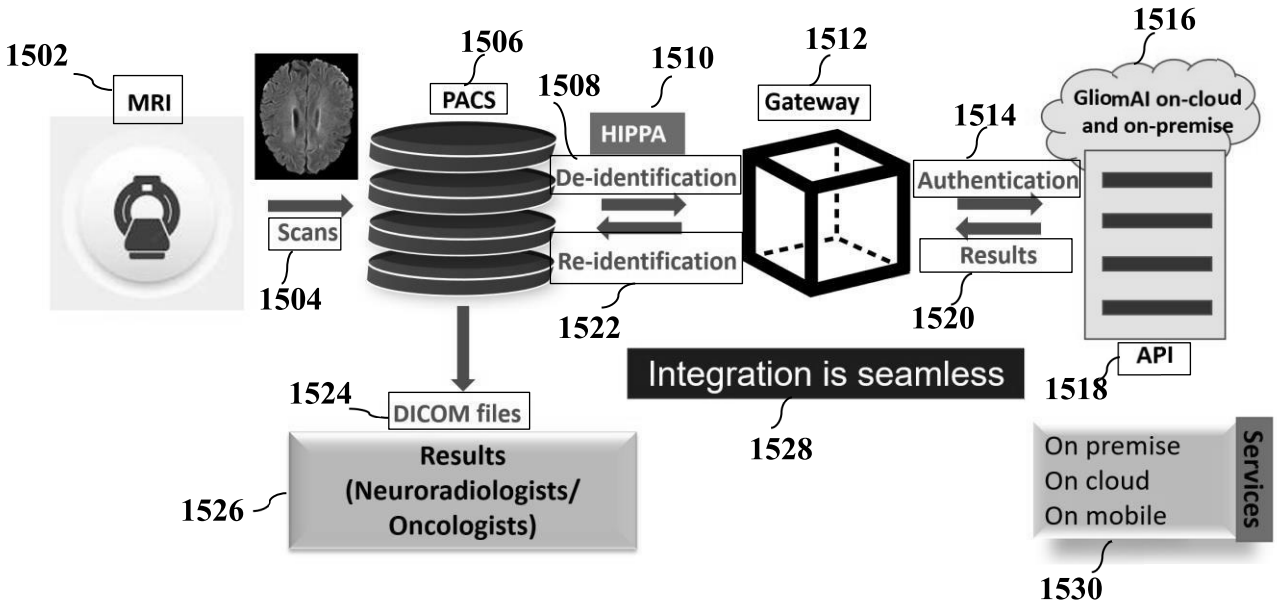


FIG. 15

Signature: -Sd-

Name: Dr Lipika Sahoo

Registration Number: IN/PA 2467

Agent for Applicant

This document is signed with the digital signature of patent agent Dr Lipika Sahoo Registration Number: IN/PA 2467

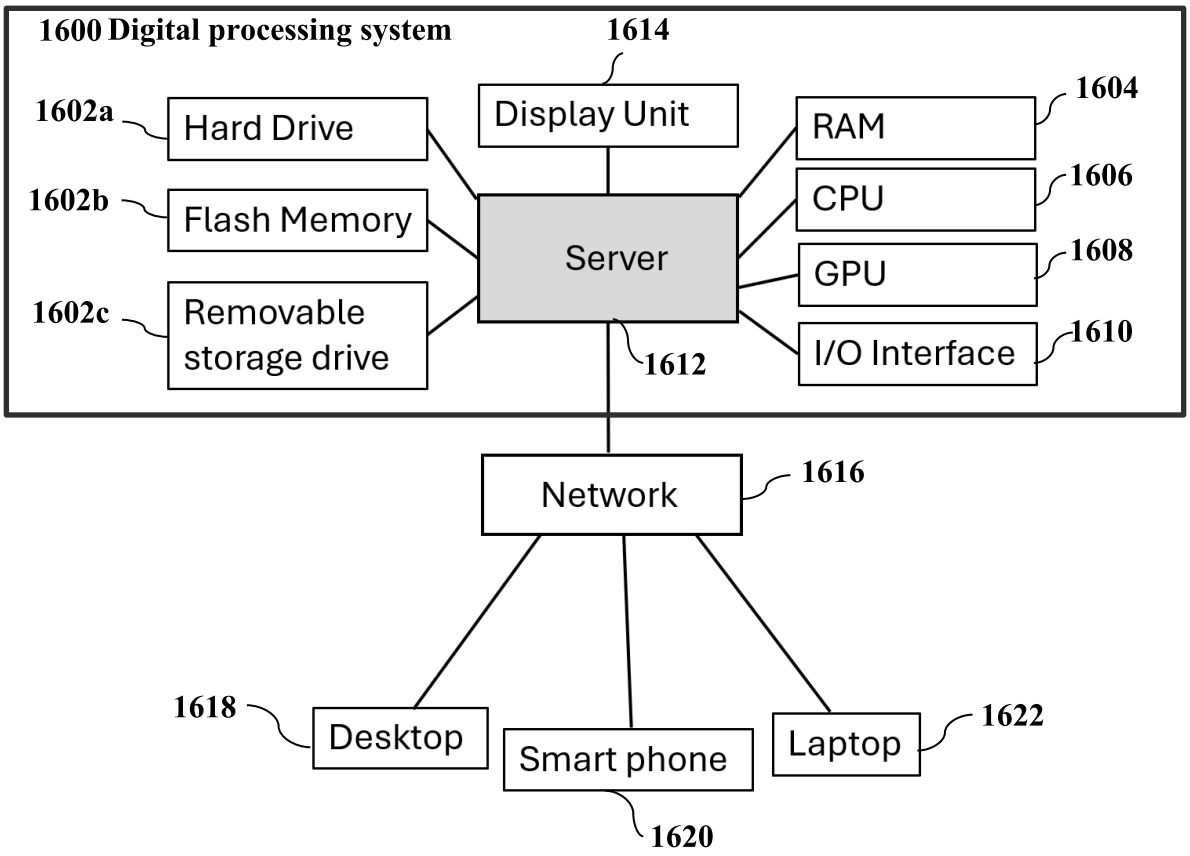


FIG. 16

Signature: -Sd-
Name: Dr Lipika Sahoo
Registration Number: IN/PA 2467
Agent for Applicant

This document is signed with the digital signature of patent agent Dr Lipika Sahoo Registration Number: IN/PA 2467

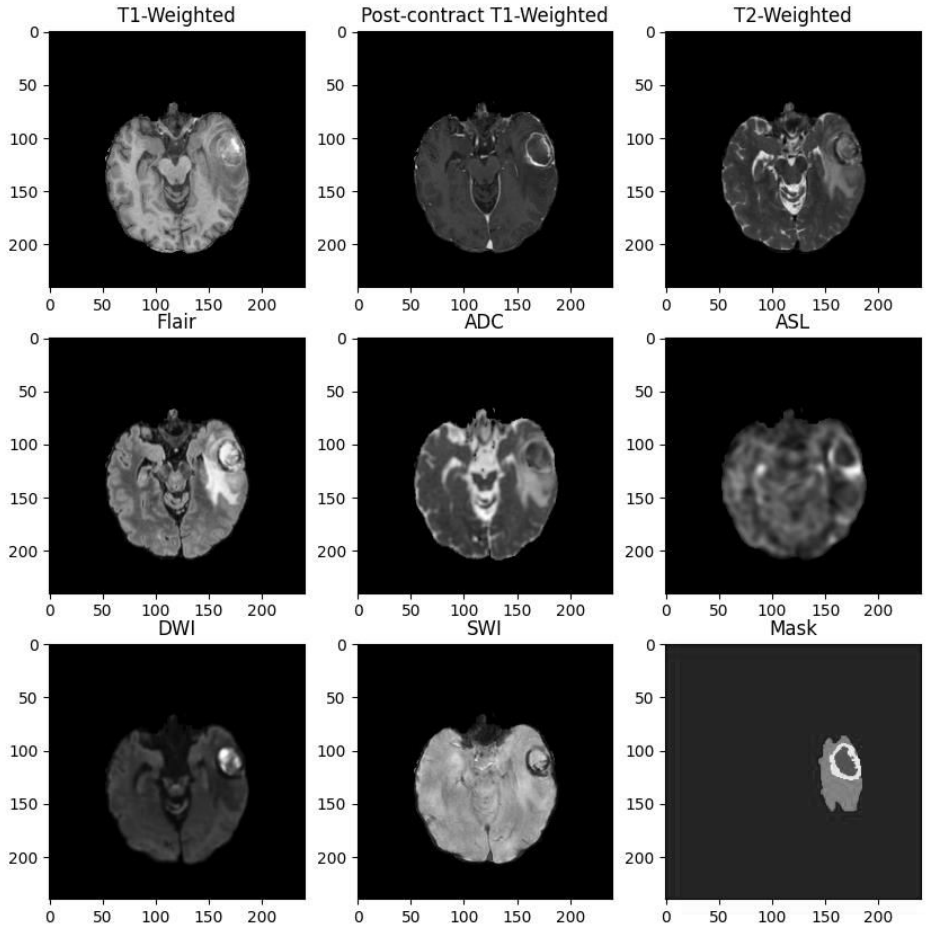


FIG. 1

Signature: -Sd-
(Lipika Sahoo)
Registration Number: IN/PA 2467
Agent for Applicant

This document is signed with the digital signature of Patent Agent [LIPIKA SAHOO (IN/PA-2467)] for the Applicant.

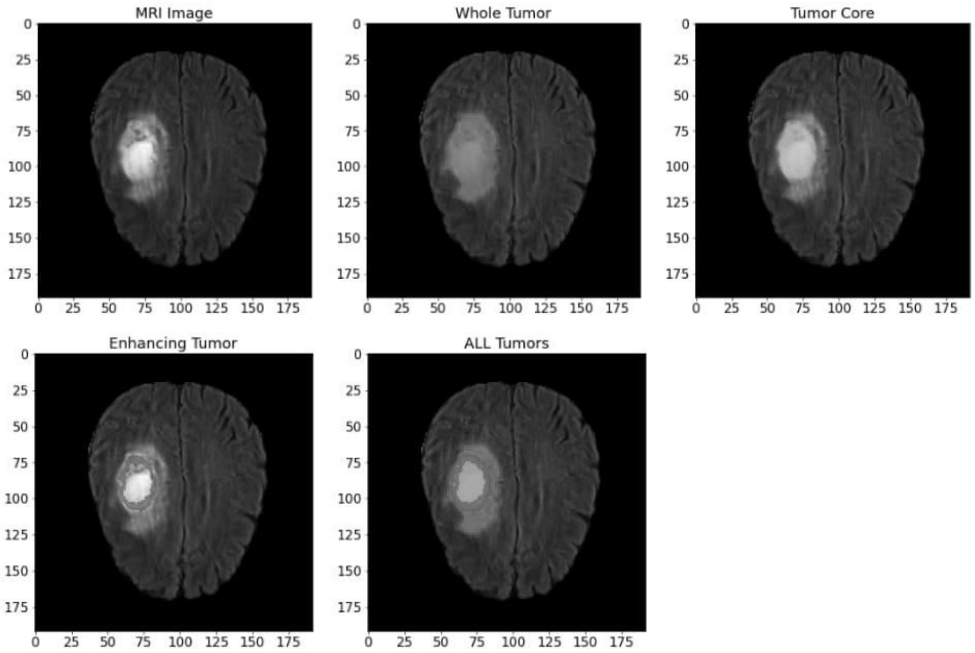


FIG. 2.

Signature: -Sd-
(Lipika Sahoo)
Registration Number: IN/PA 2467
Agent for Applicant

This document is signed with the digital signature of Patent Agent [LIPIKA SAHOO (IN/PA-2467)] for the Applicant.

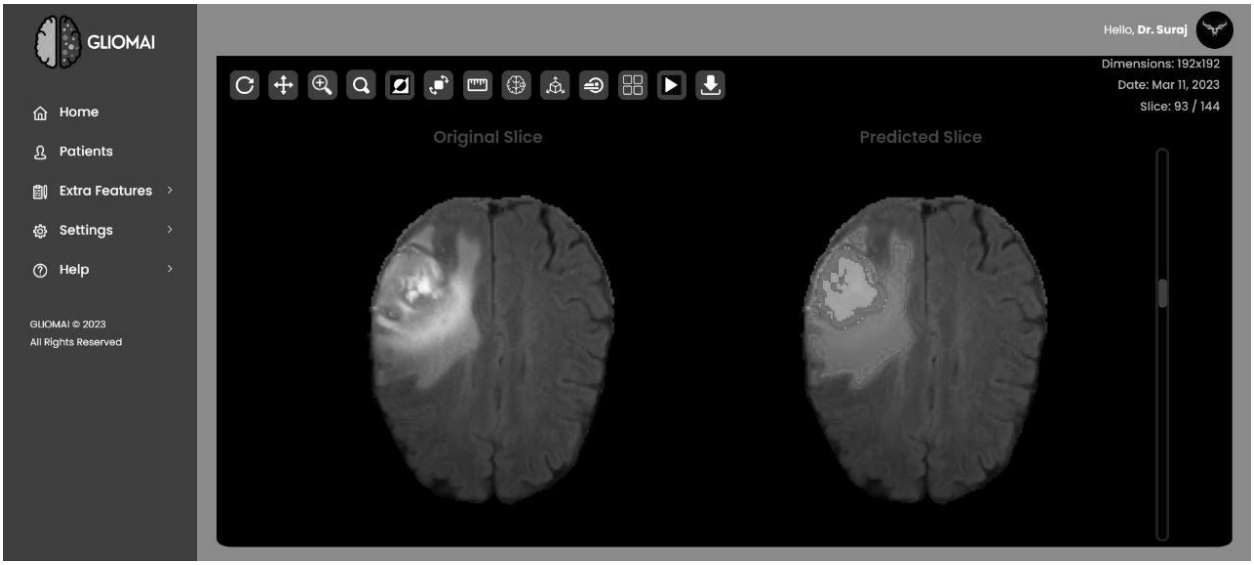


FIG. 3.

Signature: -Sd-
(Lipika Sahoo)
Registration Number: IN/PA 2467
Agent for Applicant

This document is signed with the digital signature of Patent Agent [LIPIKA SAHOO (IN/PA-2467)] for the Applicant.

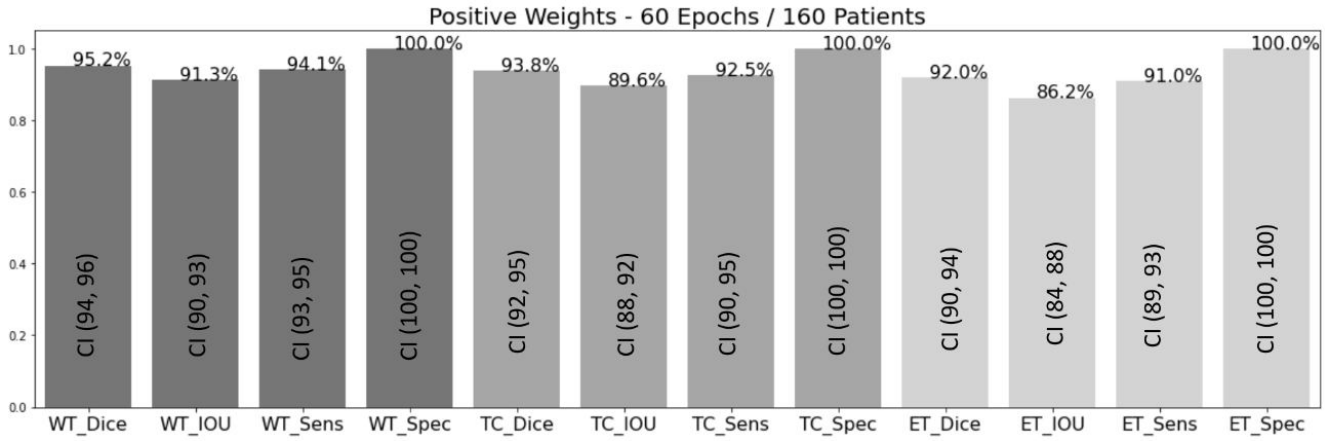


FIG. 4

Signature: -Sd-
(Lipika Sahoo)
Registration Number: IN/PA 2467
Agent for Applicant

This document is signed with the digital signature of Patent Agent [LIPIKA SAHOO (IN/PA-2467)] for the Applicant.

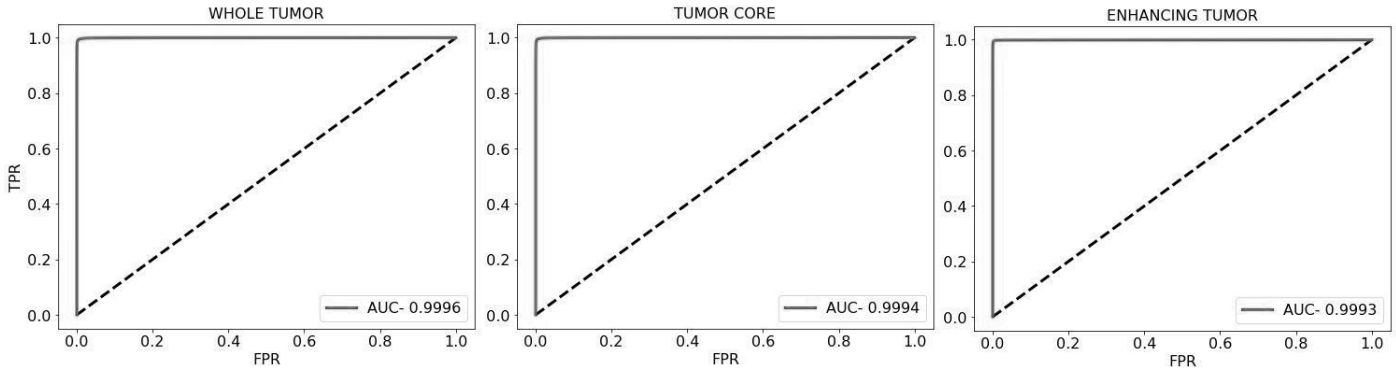


FIG. 5

Signature: -Sd-
(Lipika Sahoo)
Registration Number: IN/PA 2467
Agent for Applicant

This document is signed with the digital signature of Patent Agent [LIPIKA SAHOO (IN/PA-2467)] for the Applicant.

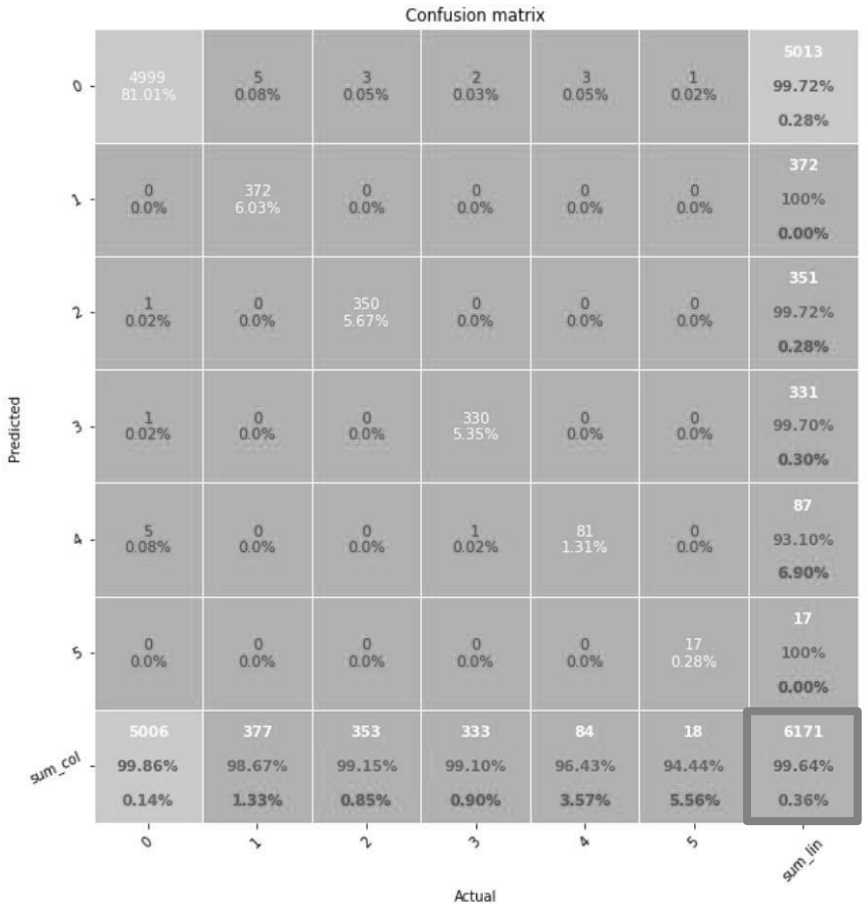


FIG. 6

Signature: -Sd-
(Lipika Sahoo)
Registration Number: IN/PA 2467
Agent for Applicant

This document is signed with the digital signature of Patent Agent [LIPIKA SAHOO (IN/PA-2467)] for the Applicant.

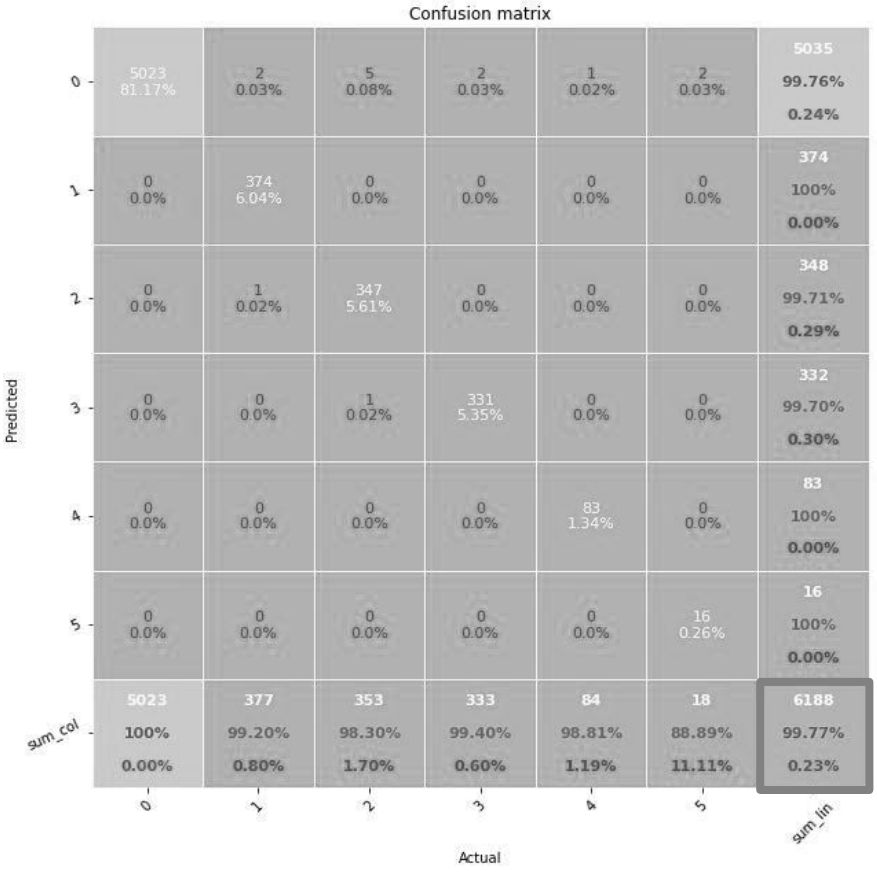


FIG. 7

Signature: -Sd-
(Lipika Sahoo)
Registration Number: IN/PA 2467
Agent for Applicant

This document is signed with the digital signature of Patent Agent [LIPIKA SAHOO (IN/PA-2467)] for the Applicant.

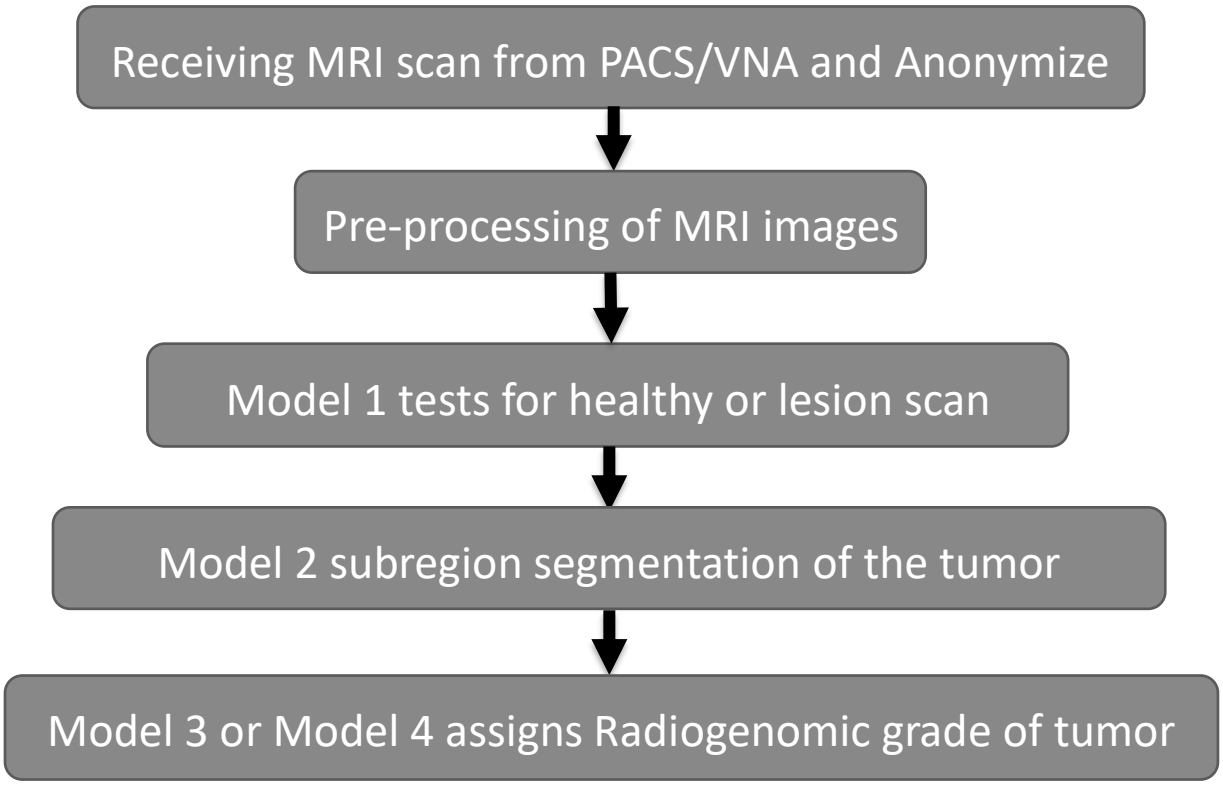


FIG. 8

Signature: -Sd-
(Lipika Sahoo)
Registration Number: IN/PA 2467
Agent for Applicant

This document is signed with the digital signature of Patent Agent [LIPIKA SAHOO (IN/PA-2467)] for the Applicant.

F O R M 2

THE PATENTS ACT, 1970

(39 of 1970)

&

THE PATENTS RULES, 2003

COMPLETE SPECIFICATION

[See section 10 and rule 13]

1. TITLE OF THE INVENTION: **NEUROIMAGING ANALYTICS AND AI- DRIVEN SYSTEM FOR GLIOMAS CLASSIFICATION USING MULTIPARAMETRIC MAGNETIC RESONANCE IMAGING**

2. APPLICANT **(A) NAME: IQSOFT TECHNOLOGIES PVT. LTD.**

(B) ADDRESS: 112, SRADDHA PALMERA, PANATHUR, BENGALURU, KARNATAKA-560037, INDIA.

3. **NATIONALITY (C) INDIA**

THE FOLLOWING SPECIFICATION PARTICULARLY DESCRIBES THE INVENTION AND THE MANNER IN WHICH IT IS TO BE PERFORMED

PRIORITY CLAIM

[001] The instant patent application is related to and claims priority from the India provisional patent application entitled, "**RADIOGENOMIC DIAGNOSIS AND PROGNOSTIC EVALUATION OF GLIOMAS**", Patent Application no.: 202341024010, Filed on: 30 March 2023, which is incorporated in its entirety herewith.

BACKGROUND OF THE DISCLOSED EMBODIMENT

[002] Technical field

[003] The present disclosure is in the technical field of artificial intelligence assisted radiogenomic classification of gliomas into isocitrate dehydrogenase (IDH) subtypes and magnetic resonance imaging (MRI) analytics for pre-operative surgical planning. More particularly, it relates solving tumor localization, volumetric quantification and classification of adult diffuse gliomas which is the most common primary brain tumor.

[004] Related art

[005] Adult diffuse gliomas are the most common primary Brain and Central Nervous System (CNS) tumor in adults which accounts for 2% of all malignant cancers that is approximately 5-10 cancer patients per 100,000 population (*Cancers 2008, 113: 1953-68; CA Cancer J Clin 2018, 68: 394-424; CA Cancer J Clin* 2021;71:381–406).

[006] According to WHO 2021 classification, gliomas are categorized into several subtypes based on molecular features and histologic characteristics such as glioblastoma or IDH wildtype, astrocytoma or IDH mutant without 1p19q codeletion and oligodendroglioma or IDH mutant with 1p19q codeletion. Low-grade gliomas display benign nature while high-grade gliomas are aggressive and have worse prognosis with 90% recurrence rate. The five-year survival rate for highly aggressive IDH wildtype (glioblastoma multiforme) is as low as 5% with a median survival time of about 12 to 18 months. The prognostic outcomes of the patients with oligodendroglioma are better than astrocytoma (Ohgaki et al, 2005 J Neruopath Expt Neurology, 51, 344-362). The survival time of low-grade gliomas

with IDH mutation and with and without 1p19q codeletion is about 10 to14 years which is much higher than glioblastoma. Studies have shown that this type of low-grade gliomas respond well to the radiation therapy and/or chemotherapy (J Neuro-Oncol (2018) 139(3):563–71.; Cancer Res (2015) 75(22):4790–802.).

[007] In the conventional method, often the exact region of interest (ROI) which represents the active tumor core in IDH subtypes of the tumor is not clearly identifiable and presence of adjoining fiber tracts further complicates the process, making it difficult to dissect tumor core and the periphery area without affecting fiber tracts. Fiber tracts controls cognitive process, motor functions and reflexive movement of muscles. To facilitate high precision tumor resection, neurosurgeon has to assess the exact location in terms of proximity to fiber tracts, volume of tumor subregions, and IDH subtypes of gliomas preoperatively and intraoperatively. That level of support and assistance is lacking in current clinical practice.

[008] Oncologists often rely on heterogeneous data sources including qualitative information from histology (e.g., morphological information) and quantitative information from genetic data (e.g., molecular information) to predict clinical outcomes. In fact, histology-based subjective and qualitative analysis of the tumor microenvironment coupled with quantitative examination of genomic assays is the standard-of-care for most cancers in modern clinical settings, but the histopathology and genetic analysis are performed separately. Present days clinical practice relies on concatenation of extracted features, which have only demonstrated marginal improvement compared to traditional analytics.

[009] Therefore, there is urgent need to precisely identify tumor subregions, its proximity to the crucial fiber tracts and the IDH subtypes automatically and non-invasively in a more reproducible manner. This is feasible by building deep learning (DL) and machine learning (ML) models which extract histologic and molecular features and deduce classification of adult diffuse gliomas into IDH subtypes non-invasively and efficiently.

[010] Prior art documents

[011] PATENT US 20210241027 discloses an image segmentation method is provided for a computing device. The method includes obtaining a general tumor

image, performing tumor localization on the tumor image to obtain a candidate image indicating a position of a tumor region in the general tumor image, inputting the candidate image to a cascaded segmentation network constructed based on a machine learning model, and performing image segmentation on the general tumor region in the candidate image using a first-level segmentation network and a second-level segmentation network in the cascaded segmentation network to obtain a segmented image.

[012] PATENT US9739783 discloses about devices and systems for diagnosing and characterizing cancer in a subject. Devices include microfilters and microfiltration systems useful for the isolation and characterization of cells from a subject.

[013] PATENT WO2020161686A1 discloses about compositions and method of cancer targeting and prognosis. The methods rely on the expression profile of 55 O-glycan forming GT (OGFGT) genes in multi-dimensional space. It was sufficient to classify cancer types from the cancer patient samples. These OGFGT genes are used to distinguish between normal and cancer samples and cancer subtypes promoting huge potential of utilizing this set of genes in diagnostic applications. The expression signature of OGFGT genes can also be used to determine survival profiles in samples from glioblastoma patients.

[014] Therefore, the said disclosure overcomes all the limitations of available prior arts.

[015] None of prior art discloses about the use of multiparametric MRI (mpMRI) images as inputs to train the DL and ML algorithms for automatic tumor subregion segmentation and concomitantly classification of gliomas into IDH subtypes based on the most significant radiogenomic features.

SUMMARY OF THE DISCLOSED EMBODIMENT

[016] The primary objective of the present disclosure is to provide automated tumor subregion segmentation, simultaneously generation of tractography, brain parcellation and classification of adult diffuse gliomas into IDH subtypes from pre-

operative multiparametric MRI scans using DL, ML and various mathematical algorithms.

[017] According to an aspect of the disclosure, a method (FIG. 2) for gliomas classification, the method comprising: receiving (202) a magnetic resonance imaging (MRI) image of a glioma patient; pre-processing (102, 208) the MRI image to obtain a processed MRI image (120) of the glioma patient; identifying (210) subregion segmentations of the gliomas in the processed MRI image, each subregion segmentations are one of peritumoral edema, enhancing tumor, non-enhancing tumor, or necrotic tumor (212); determining (220) a classification of the gliomas based on features extracted from the segmented subregions, the classification comprises isocitrate dehydrogenase (IDH) subtypes which include glioblastoma, astrocytoma and oligodendroglioma (222); and providing a visualization GUI for the segmented subregions of the gliomas and its classification into IDH subtypes.

[018] According to another aspect of the disclosure, the MRI images are multiparametric comprising of T1-weighted (T1w), T2-weighted (T2w), post-contrast-T1 weighted (T1ce) and fluid attenuated inversion recovery (FLAIR), and diffusion weighted imaging (DWI), the MRI image is in Digital Imaging and Communications in Medicine (DICOM) format.

[019] According to one more aspect of the disclosure, the pre-processing (102, 208) comprises one or more of deidentification (104), conversion of the MRI image to Neuroimaging Informatics Technology Initiative (NIfTI) format (106), motion correction (108), BIAS correction (110), noise reduction (112), registration and resampling of the 3D volume of the MRI image (114), skull stripping (116) and normalization (118).

[020] According to yet another aspect of the disclosure, the method comprising:

a) training a segmentation Artificial Intelligence (AI) module (210) using a deep learning (DL) technique to correlate various portions of MRI images to subregion segmentations of gliomas,

b) the identifying comprises providing the processed MRI image as input to the segmentation AI module to obtain as output subregion segmentations of the gliomas in the processed MRI image.

[021] According to the further aspect of the disclosure, the method comprising:

a) training a classification AI module (220) using a ML/DL technique to correlate features of the subregion segmentations of gliomas to classifications of gliomas,

b) the determining comprises:

extracting (216) a set of features from the segmented subregions of the gliomas, the features include Visually Accessible Rembrandt Images (VARARI) features, radiomic features and clinical information;

c) selecting (218) a subset of significant features from the set of features, the feature selection eliminates redundant features; and

d) provides the subset of significant features as input to the classification AI module to obtain the classification of the gliomas as output.

[022] According to an aspect of the disclosure, comprising deducing (214) volumetric quantifications for each segmented subregion of the gliomas.

[023] According to another aspect of the disclosure, comprising generating (402) a report including one or more of volume of the subregion segmentations (404), differentiation between peritumoral edema and tumor core (406), location of the gliomas (408), identification of the fiber tracts presents in close contact with the gliomas (410), textural features of the gliomas (412) and IDH subtypes of the gliomas (416).

[024] According to an aspect of the disclosure, a neuroimaging analytics and AI-driven system for gliomas classification (FIG. 3), the system comprising:

a) a pre-processing (306) module configured to receive a magnetic resonance imaging (MRI) image of a gliomas and to pre-process the MRI image to obtain a processed MRI image (120) of the gliomas;

b) a segmentation Artificial Intelligence (AI) module (210, 316) configured to identify segmented subregions of the gliomas in the processed MRI image, each subregion is a peritumoral edema, enhancing tumor, non-enhancing tumor, or necrotic tumor (212);

c) a classification AI module (220, 318) configured to determine a classification of the gliomas based on the features selected from the subregions of gliomas, the classification comprises isocitrate dehydrogenase (IDH) subtypes such as glioblastoma, astrocytoma and oligodendroglioma (222); and

d) a brain parcellation module (310) performs parcellation based on predefined atlas; and

e) a tractography map (314) of the brain generated from dMRI to visualize fiber tracts adjacent to the tumor;

and obtaining textural feature (312) of the tumor for reporting and also the training of classification model; and

f) a visualization module configured to provide a visualization (320) of the subregion segmentations of the gliomas and the classification.

[025] According to another aspect of the disclosure, the neuroimaging analytics and AI-driven system of, the segmentation AI module (210) is trained using a ML/DL technique to correlate various portions of MRI images to subregion segmentations of gliomas,

The segmentation AI module is configured to receive the processed MRI image as input and provides segmented subregions as the output from the processed MRI image of the glioma patient.

[026] According to yet another aspect of the disclosure, the neuroimaging analytics and AI-driven system, the classification AI module (220) is trained using a ML/DL technique to correlate features of the subregion segmentations of gliomas to classifications of gliomas,

the system is configured to:

a) extract (216) a set of features from the subregion segmentations of the gliomas, wherein the features include Visually Accessible Rembrandt Images (VARARI) features and clinical information;

b) select (218) a subset of significant features from the set of features, wherein the selection also eliminates redundant features; and

provide the subset of significant features as input to the classification AI module to obtain an output of gliomas classification.

[027] Several aspects of the disclosed embodiment are described below with reference to examples for illustration. However, one skilled in the relevant art will recognize that the disclosed embodiment can be practiced without one or more of the specific details or with other methods, components, materials and so forth. In other instances, well-known structures, materials, or operations are not shown in detail to avoid obscuring the features of the disclosed embodiment. Furthermore, the features/aspects described can be practiced in various combinations, though only some of the combinations are described herein for conciseness.

BRIEF DESCRIPTION OF THE DRAWINGS

[028] Example embodiments of the disclosed embodiment is described with reference to the accompanying drawings briefly as follows.

[029] **FIG. 1** illustrates the modules used for preprocessing of the MRI images, according to the aspect of the disclosed embodiment.

[030] **FIG. 2** illustrates the scheme of the AI modules which include tumor subregion segmentation module and classification into IDH subtypes module in adult diffuse gliomas, according to the aspect of the disclosed embodiment.

[031] **FIG. 3** illustrates the scheme for overall process of neuroimaging analytics, AI-assisted modules for assessment and visualization of brain tumor, according to the aspect of the disclosed embodiment.

[032] **FIG. 4** illustrates the important findings which appears in a report format resulted from the brain MRI image analytics, according to the aspect of the disclosed embodiment.

[033] **FIG. 5** MRI sequences of the patients and the annotated tumor subregions of glioblastoma (top panel), astrocytoma (middle panel) and oligodendroglioma (bottom panel), according to the aspects of the disclosed embodiment.

[034] **FIG. 6** illustrates the segmented regions or ROI resulted from the DL model such as whole tumor (WT), tumor core (TC) and enhancing tumor (ET) which are used to delineate peritumoral edema, enhancing tumor and non-enhancing or necrotic core, according to the aspects of the disclosed embodiment.

[035] FIG. 7 illustrates Dice coefficient, Jaccard index or Intersection over Union (IoU), sensitivity and specificity of WT (blue), TC (pitch) and ET (green) in bar plots, according to the aspects of the disclosed embodiment.

[036] FIG. 8 illustrates Receiver Operating Curves (ROC) of WT, TC and ET showing area under the curve (AUC), according to the aspects of the disclosed embodiment.

[037] FIG. 9 illustrates comparison of volumetric information of WT, TC and ET between radiologist annotation and AI model prediction for the glioma patients, according to the aspects of the disclosed embodiment.

[038] FIG. 10 illustrates anatomical parcellation of brain as per Talairach brain atlas according to the aspect of the disclosed embodiment.

[039] FIG. 11 illustrates location and proximity of the segmented tumor and white matter fiber tracts in 3D brain space of patient, according to the aspect of the disclosed embodiment.

[040] FIG. 12 illustrates 3D fiber bundles and annotated tumor on 2D slice of T1w MRI image, according to the aspect of the disclosed embodiment.

[041] FIG. 13 illustrates the bar plots showing mean and standard deviation of accuracy, F1 score, sensitivity and specificity of the adult diffuse gliomas classification performed using random forest (RF), logistic regression (LR), decision tree (DT), support vector classifier (SVC) and XGBoost (XGB), according to the aspects of the disclosed embodiment.

[042] FIG. 14 illustrates GUI application for performing neuroimaging analytics and visualization of neuroimages, according to the aspects of the disclosed embodiment.

[043] FIG. 15 illustrates deployment workflow, according to the aspects of the disclosed embodiment.

[044] FIG. 16 illustrates a block diagram illustrating the details of a digital processing system in which various aspects of the disclosed embodiment are operative by execution of appropriate execution modules, firmware, or hardware components, according to the aspects of the disclosed embodiment.

[045] In the drawings, like reference numbers generally indicate identical, functionally similar, and/or structurally similar elements. The drawing in which an element first appears is indicated by the leftmost digit(s) in the corresponding reference number.

DETAILED DESCRIPTION OF THE DISCLOSED EMBODIMENT

[046] It is to be understood that the present disclosure is not limited in its application to the details of construction and the arrangement of components set forth in the following description or illustrated in the drawings. The present disclosure is capable of other embodiments and of being practiced or of being carried out in various ways. Also, it is to be understood that the phraseology and terminology used herein is for the purpose of description and should not be regarded as limiting.

[047] The use of “including”, “comprising” or “having” and variations thereof herein is meant to encompass the items listed thereafter and equivalents thereof as well as additional items. The terms “a” and “an” herein do not denote a limitation of quantity, but rather denote the presence of at least one of the referenced items. Further, the use of terms “first”, “second”, and “third”, and the like, herein do not denote any order, quantity, or importance, but rather are used to distinguish one element from another. Further, the terms “comprising,” “including,” “having,” and the like, as used with respect to embodiments of the present disclosure, are synonymous.

[048] Alternative embodiments of the present disclosure and their equivalents may be devised without parting from the spirit or scope of the present disclosure. It should be noted that any discussion herein regarding “one embodiment”, “an embodiment”, “an exemplary embodiment”, and the like indicate that the embodiment described may include a particular feature, structure, or characteristic and that particular feature, structure, or characteristic may not necessarily be included in every embodiment. In addition, references to the foregoing do not necessarily comprise a reference to the same embodiment. Finally, irrespective of whether it is explicitly described, one of ordinary skill in the art would readily appreciate that each of the particular features, structures, or characteristics of the

given embodiments may be utilized in connection or combination with those of any other embodiment discussed herein.

[049] As used herein, the singular forms “a”, “an”, and “the” include both singular and plural referents unless the context clearly dictates otherwise.

[050] The terms “comprising”, “comprises” and “comprised of” as used herein are synonymous with “including”, “includes” or “containing”, “contains”, and are inclusive or open-ended and do not exclude additional, non-recited members, elements or method steps.

[051] All documents cited in the present specification are hereby incorporated by reference in their totality. In particular, the teachings of all documents herein specifically referred to are incorporated by reference.

[052] Example embodiments of the disclosed embodiments are described with reference to the accompanying figures.

[053] DEFINITIONS

[054] The term ‘Brain tumor’ refers to a cancerous or non-cancerous mass or growth of abnormal cells in the brain.

[055] The term “Glioma” refers to a growth of cells that starts in the brain or spinal cord. The cells in a glioma look similar to healthy brain cells called glial cells. Glial cells surround nerve cells and help them function. As a glioma grows it forms a mass of cells called a tumor.

[056] The term “Glioblastoma” refers to a type of cancer that starts as a growth of cells in the brain or spinal cord. It grows quickly and can invade and destroy healthy tissue. Glioblastoma forms from cells called astrocytes that support nerve cells. These are IDH wildtype.

[057] The term “Astrocytoma” refers to a kind of cancer that originates in glial cells are known as astrocytes and are developed in the brain or spinal cord. It starts in the astrocytes, which are cells that support nerve cells. While some astrocytomas grow relatively slowly, others may develop into malignant tumors that spread swiftly. These are IDH mutant without 1p19q codeletion.

[058] The term “oligodendroglioma” refers to a rare kind of brain tumor known as an oligodendroglioma arises from glial cells known as oligodendrocytes. Adults

are more likely than children to have it. The location of the tumor in the brain determines the symptoms of oligodendroglioma. These are IDH mutant with 1p19q codeletion.

[059] The term "MRI" refers to a magnetic resonance imaging (MRI) scan uses a strong magnetic field and radio waves to create detailed images of the organs and tissues within the body. MRI helps in viewing soft tissue with better contrast with no radiation exposure and thus are commonly used to visualize brain injuries, tumors, stroke, epilepsy, Alzheimer, developing brain and many more.

[060] 1. EMBODIMENTS OF THE DISCLOSURE

[061] The goal of present disclosure is to perform auto-preprocessing, conversion into any type of MNI space brain atlas depending upon the need, generation of tractography map, auto-segmentation of tumor into distinct subregions, extraction of radiomic textural features and classification of gliomas into IDH subtypes.

[062] 2. PROCESS FOR NEUROIMAGING ANALYTICS AND CLASSIFICATION OF GLIOMAS INTO IDH SUBTYPES

[063] The process of gliomas segmentation and classification is carried out systematically following a defined procedure accompanied by neuroimaging analytics. The embodiment herein and various other features are explained more fully with references in the accompanying drawing and the details in the following descriptions.

[064] The detection procedure begins by receiving an MRI image from picture archiving and communication system (PACS). The image is preprocessed automatically **(102)** by one or more modules as shown in **FIG. 1**. (**104)** module performs deidentification as per HIPPA compliance which protect patient privacy. The DICOM files are then converted to Neuroimaging Informatics Technology Initiative (NIfTI) format by the module (**106)** and its corresponding headers into JSON format. The module (**108)** performs motion correction, (**110)** does BIAS correction and (**112)** performs noise correction. 3D volume is co-registered to a common anatomical template SRI24 and resampled to 1 mm^3 **(114)**. Skull stripping is performed by an inhouse developed trained model of present disclosure which has dice coefficient of 98%, Jaccard index 97%, sensitivity 98% and specificity

100%. Subsequently normalization is performed by the module (**118)** to achieve the processed image **(120)**.

[065] **FIG. 2** shows the workflow carried out by AI modules. It receives multiparametric MRI images **(202)** in DICOM format which are deidentified **(204)** as per HIPPA compliance **(206)** and undergoes preprocessing **(208)** as shown in **(FIG. 1).** The processed images are fed into AI modules which performs Task 1 that is tumor subregion segmentation **(210)** of gliomas into peritumoral edema, enhancing tumor, non-enhacing or nacrotic tumor **(212)**. Volumetric quantifications **(214)** are deduced for these subregions. This is an important method for carrying out one or more clinical processes such as pre-operative surgical planning, radiation therapy planning, neuronavigator feed to be used as intra-operative guidance. The segmented subregions are used for features extraction which also include Visually Accessible Rembrandt Images (VARARI) features and clinical information **(216)**. More than four thousand of features are considered which are subjected to feature selection algorithm **(218)** to limit the number of features to few hundreds which represents the significant features. This step eliminates the redundant features. The features are trained in Task 2 **(220)** to classify gliomas into IDH subtypes which are glioblastoma, astrocytoma and oligodendroglioma **(222)**. Identification of IDH subtypes has important implications in subsequent adjuvant therapy which is different for different IDH subtypes. The AI modules **(224)** follow a continuous training protocol to update the models with the addition data. Therefore, there is a feature of continuous adaptive learning **(226)**. The AI modules are integrated into our application and is used for preoperative neuroanalytics and assessment of the tumor **(228)**.

[066] According to an embodiment as shown in **FIG. 3**, medical images are stored in a database **(302)** that is PACS. Multiparametric MRI (mpMRI) images **(304)** such as T1w, T2w, T1ce and FLAIR, diffusion weighted imaging (DWI) are pre-processed **(306)**. To perform brain parcellation, the preprocessed image is transformed into MNI space **(308)** and then parcellation **(310)** is performed following the template atlas as per the requirement. The preprocessed image can also undergo filtering and feature extraction **(312)**. T1w image is subjected to

anatomical brain parcellation. Diffusion MRI (dMRI) that is diffusion tensor imaging (DTI) is used to provide personalized brain map called tractography **(314)** which is critical for locating the brain connections and for accessing information of the tissue microstructure. Structural MRI such as T1w, T2w, T1ce and FLAIR are used for tumor subregions delineation **(316)**. Tractography in combination with tumor segmentation provides automatic identification of important fiber tracts along with precise location of the tumor which serves as indispensable tool for neurosurgical guidance. Preoperative planning with the aid of tractography and tumor localization protects eloquent brain functions such as critical motor, visual, language and somatosensory functions which are linked via the tracts. Further, the AI modules perform radiogenomic classification **(318)** which assigns IDH subtypes to adult diffuse gliomas. The results are visualized via Graphical User Interface (GUI) based web application built inhouse **(320)**. This embodiment explains complete flow of connected modules which can be executed independently or in a dependent manner.

[067] In an embodiment, the report generated **(402)** by the application as shown in **FIG.4** includes volume of the tumor subregions **(404)** which are differentiated as peritumoral edema and tumor core **(406)**. It provides location of the tumor **(408)** and identify the fiber tracts present in close contact with the tumor **(410)**. The report also delineates textural features of the tumor **(412)** and provides IDH subtype non-invasively **(416) (FIG. 4).**

[068] 3. STRUCTURAL MRI SEQUENCES OF THE PATIENTS AND THE ANNOTATED TUMOR SUBREGIONS

[069] This embodiment in **FIG. 5,** the MRI sequences of the patients T1w **(502)**, T2w **(504)**, T1ce **(506)** and FLAIR **(508)** of glioblastoma (top panel) **(510)** astrocytoma (middle panel) **(512)** and oligodendroglioma (bottom panel) **(514)** and the corresponding annotated tumor subregions **(516)**. These images are used to train the tumor segmentation model. Three distinct color codes green, yellow and red colours are used to indicate peritumoral edema **(518)**, enhancing tumor **(520)** and non-enhancing and/or necrotic tumor core regions **(522)** respectively**.** Annotation of tumor subregions are performed by algorithms and manually corrected by expert

neuroradiologists and are used as the ground truth. Segmentation model is trained, validated, and tested using a large dataset of 2901 glioma patients totalling to 17, 98, 620 MRI image slices.

[070] 4. SEGMENTED SUBREGIONS OF THE GLIOMAS

[071] The segmented subregions of the gliomas, the top panel of **FIG. 6** shows three distinct subregions **(602)**, the WT **(604)**, TC **(606)** and ET **(608)** predicted by our tumor segmentation model. The bottom panel indicates the subregions **(610)** which are delineated from WT, TC and ET into peritumoral edema **(612),** enhancing tumor **(614)** and non-enhancing or necrotic core **(616)**.

[072] For tumor segmentation, T1w, T2w, T1ce, and FLAIR MRI images are used. For the purpose, the entire dataset is divided into training-validation set (80%) and test set (20%) and subsequently training-validation set is further spitted to training set (70%) and validation set (10%) using StratifiedKFold cross-validation where K=5.

[073] The present disclosure employs loss function to train the model. It uses a modified U-Net architecture. Training and validation loss function is plotted as a function of epochs. Performance on validation set is used as a criterion to select the best model. The chosen model is then tested on four test sets obtained from different scanners and institutions. The test dataset A having 210 patients, dataset B having 97 patients, dataset C having 39 patients and dataset D having 611 patients. DICE coefficient, Jaccard index, sensitivity and specificity are determined for WT (blue), TC (pitch) and ET (green) **(FIG 7A, B, C, and D).** Present disclosure obtained dice coefficient, IoU, sensitivity and specificity greater than 95, 87, 90, 99% for WT, 90, 83, 91,100% for TC and 85, 76, 88, 100% for ET respectively tested on dataset A. For B, C, D test sets results are shown in **FIG. 7B, C, C.**

[074] Present discloser shows AUC on ROC for the WT, TC and ET in **FIG. 8** which are observed to be 100% for the dataset A and B suggesting high fidelity performance of the model in delineating the tumor subregions across the different threshold values. Mean and 95% confidence interval (CI) is calculated for each metric for all the datasets are shown in Table 1.

[075] FIG. 9 in the present disclosure shows the comparison of the neuroradiologists annotated WT, TC and ET regions with our model delineated regions. There is an excellent agreement in volumetric quantification indicating robust performance of the model.

[076] Table 1. Performance evaluation of tumor segmentation model on four test sets.

Dataset A					
Tumor subregions	# Patient	DICE (95% CI)	IOU (95% CI)	Sensitivity (95% CI)	Specificity (95% CI)
WT	210	0.9273 (0.9156-0.9390)	0.8729 (0.8581-0.8877)	0.9164 (0.9022-0.9305)	0.9993 (0.9992-0.9994)
TC	210	0.8697 (0.8389-0.9004)	0.8157 (0.7837-0.8476)	0.8777 (0.8474-0.9081)	0.9996 (0.9995-0.9997)
ET	210	0.8214 (0.7887-0.8541)	0.7449 (0.7124-0.7774)	0.8308 (0.7857-0.8521)	0.9996 (0.9996-0.9997)
Dataset B					
WT	97	0.9301 (0.9219-0.9384)	0.8720 (0.8584-0.8856)	0.9164 (0.9018-0.9311)	0.9991 (0.9990-0.9993)
TC	97	0.9011 (0.8816-0.9206)	0.8311 (0.8051-0.8572)	0.9107 (0.8919-0.9295)	0.9992 (0.9990-0.9995
ET	97	0.8593 (0.8407-0.8778)	0.7635 (0.7377-0.7892)	0.8861 (0.8676-0.9045)	0.9992 (0.9989-0.9994)
Dataset C					
WT	39	0.9606	0.9253	0.9907	0.9982

		(0.9525-0.9688)	(0.9107-0.9400)	(0.9869-0.9944)	(0.9977-0.9988)
TC	39	0.9637 (0.9454-0.9821)	0.9348 (0.9058-0.9637	0.9995 (0.9992-0.9998)	0.9991 (0.9985-0.9997)
ET	39	0.9778 (0.9718-0.9837)	0.9571 (0.9461-0.9682)	0.9998 (0.9997-0.9999)	0.9996 (0.9995-0.9997)
Dataset D					
WT	611	0.9543 (0.9507-0.9579)	0.9158 (0.9099-0.9217)	0.9507 (0.9458-0.9556)	0.9995 (0.9994-0.9995)
TC	611	0.9422 (0.9347-0.9497)	0.9008 (0.8916-0.9101)	0.9457 (0.9373-0.9541	0.0003 (0.9998-0.9998)
ET	611	0.9015 (0.8920-0.9111	0.8357 (0.8244-0.8469)	0.9217 (0.9123-0.9311)	0.9997 (0.9997-0.9997)

[077] 5. BRAIN PARCELLATION

[078] In the present disclosure, brain parcellation is performed on the structural MRI, T1w image to understand the anatomical organization and relate it to the specific function using diffusion MRI. It plays crucial role in understanding the effects of neurological disorders, brain injuries and neurodegenerative diseases on specific brain regions or networks. It helps clinicians to identify abnormalities in brain structure and function associated with various neurological conditions and thus helps in tailoring the treatment. In neurosurgery accurate delineation of brain regions is important for planning surgical intervention. Brain parcellation helps neurosurgeons to identify critical structure and avoid damage to the eloquent brain regions responsible for language, motor control etc. Brain parcellation also been

useful in analysing and visualizing neuroimaging data and compare the result across individuals or populations to get clinical anatomical insights.

[079] Brain parcellation is performed by converting MRI image to MNI space transformation using predefined anatomical atlases such as Talairach, automated anatomical labelling (AAL), Harvard-Oxford, MNI structural atlas, Desikan-Killiany atlas. Each brain atlas has its own specifications.

[080] In the present disclosure, **FIG 10** shows brain parcellation as per Talairach brain atlas. It delineates cortical and subcortical structures. The top panel shows axial **(1002)**, sagittal **(1004)** and coronal **(1006)** views of the brain as left (purple) and right (cyan) cerebrum **(1008)**, cerebellum, brainstem and inter-hemispheric regions. Further, it segregates gray matter (red), white matter (green) and cerebro-spinal fluid (blue) **(1010)** (middle panel). Bottom panel **(1012)** differentiates various lobes of the brain as defined in Talairach atlas.

[081] 6. USAGE OF TRACTOGRAPHY IN NEUROSURGICAL GUIDANCE, UNDERSTANDING BRAIN CONNECTIVITY AND INVESTIGATING NEUROLOGICAL DISORDERS

[082] Tractography provides insights of the structural connectivity pattern of the brain which includes major fiber bundles and their spatial relationships. It provides information about how different brain regions are anatomically connected and communicate with each other through white matter pathways. Tractography is used in clinical setting to investigate various neurological disordered such as brain stroke, traumatic brain injury, epilepsy etc. Recently, tractography has been widely used in neurosurgical planning to assist neurosurgeon in delineating white matter pathways to avoid damage to critical fiber bundles during surgical interventions.

[083] In the present disclosure, combined use of segmented tumor and tractography are implicated to be used as surgical guidance. It helps neurosurgeon to visualize spatial relationships between tumor and the adjacent fiber bundles to minimize damage to the eloquent brain regions thus enabling safer and high precision surgery. **FIG. 11** in the present disclosure shows axial **(1102)**, sagittal **(1104)** and coronal **(1106)** 3D views of the brain having tumor and selected fiber bundles such as corpus callosum **(1108)**, frontopontine tract **(1110)**, corticospinal

tract **(1112)**, superior longitudinal fasciculus **(1114)** and interior fronto-occipital fasciculus **(1116)**. While many of the fiber bundles are away from the tumor, corpus callosum and interior fronto-occipital fasciculus are adjacent to the tumor. Such visualization guide neurosurgeon to safely remove the tumor without affecting the fiber tracts thus protecting the crucial brain functions.

[084] **FIG. 12** shows an example case where tumor **(1210)** and corpus callosum **(1208)** fiber tract are overlaid on the 2D plane of T1w MRI in axial **(1202)**, sagittal **(1204)** and coronal **(1206)** views.

[085] Our application can calculate the minimum distance between the tumor and all the fiber bundles and recommend the bundles for visualization which are closer making neurosurgeon's surgical planning more efficient.

[086] Visualization of tumor with fiber tracts has paramount importance in deciding the surgical corridor.

[087] There are situations when tumor growth pushes the fiber tract to one side different from original location which are invisible in structural MRI. In such situation tractography along with tumor visualisation is indispensable.

[088] There are conditions when tumor growth is in and around the fiber bundle. In such situation, the entire neurosurgical procedure changes. Instead of tumor being taken out in its entirety, it is removed in pieces.

[089] Tractography acts as surgical guidance not only for tumor but also for any lesion which can be a surgical target.

[090] 6. SEGMENTED TUMOR SUBREGIONS AS PRE-OPERATIVE AND INTRAOPERATIVE SURGICAL GUIDANCE AND USED FOR THE DEVELOPMENT OF IDH SUBTYPE CLASSIFICATION

[091] The segmented tumor subregions are used for the development of IDH subtypes classification. The classification model is built using machine learning method. This method uses clinical features of patient, qualitative and radiomic features of multiparametric MRI images and their filters. Present disclosure extracted radiomic features of first order statistics, 3D shape-based features, 2D based shape features. There are features from gray level co-occurrence matrix (GLCM), Gray level run length matrix (GLRLM), Gray level size zone matrix

(GLSZN), Neighbouring gray tone difference matrix (NGTDM) and Gray level dependence matrix (GLDM). These radiomic features are also extracted from Laplacian of Gaussian (LoG) and wavelet filters. Likewise, a total of 4904 features are selected from the four multiparametric MRI images. Subsequently, features providing redundant information are removed. The selection procedure retains only a few hundred features. These features are further subjected to feature selection algorithm. Finally, less than hundred unique features are selected which are subjected to different machine learning classifiers such as Random Forest (RF), Decision Tree (DT), Logistic Regression (LR), Support Vector Classifier (SVC), XGBoost (XGB). The best classifier is chosen based on accuracy, F1 score, sensitivity and specificity. The result obtained is shown in (**FIG. 13A, B, C, and D**) which shows Random Forest classifier's performance is relatively better than other classifiers. The accuracies are 93±3, 86±4, 90±4(%), F1 scores are 93±3, 79±6, 57±17(%), sensitivities are 96±4, 79±7, 52±16(%) and specificities are 89±4, 90±5, 96±3(%) for differentiating glioblastoma, astrocytoma and oligodendroglioma respectively with RF classifier.

[092] 6. STATISTICAL ANALYSIS

[093] Area under the ROC curve is used to determine the model's ability to distinguish different tumor classes across all possible thresholds. ROC curves are determined for WT, TC and ET subregions which are observed to be greater than 99% indicating robust performance of the segmentation model. The statistical analysis Cohen's kappa is determined for the classification model to analyze the agreement between the predicted results by our classifiers and actual result obtained from the immunohistochemistry and histopathology. The Cohen's kappa values for RF, DF, LR, SVC and XGB classifiers averaged over the five folds are 72±7, 60±7, 69±6, 69±7 and 68±7(%) respectively suggesting better performance for RF classifier. The AUCs determined from ROCs are 95, 77, 93, 94 and 91% for RF, DF, LR, SVC and XGB classifiers respectively indicating better performance of RF to classify IDH subtypes. We also determine Pearson correlation over five folds for RF, DF, LR, SVC and XGB classifiers which are 79±6, 64±6, 74±5, 77±6 and 76±5(%) respectively indicating similar finding like that Cohen's kappa statistical

measure.

[094] 7. GUI APPLICATION FOR VISUALIZATION OF TUMOR WITH PARCELLED BRAIN AND TRACTOGRAPHY ON MRI IMAGES

[095] In this disclosure a web-based GUI application is used (**FIG. 14**) for visualization of tumor subregions on structural MRIs in 2D with axial **(1402)**, sagittal **(1404)** and coronal planes **(1406)** and on 3D brain **(1408)**. The top panel **(1410)** of the GUI has several tools and options to transform the image visualization. The left side of the GUI has the menu **(1412)** to provide input MRI images for prediction and visualization of new patient data. There is a provision for brain parcellation and generation of tractography map.

[096] 8. PREOPERATIVE SEGMENTATION, CLASSIFICATION AND NEUROSURGERY GUIDANCE FOR GLIOMAS PROGNOSIS

[097] To carryout assessment of gliomas, the MRI images **(1504)** are recorded in the MRI scanner **(1502)** and scans are stored securely in PACS **(1506)** or Vendor Neutral Archives (VNA) are accessed via the gateway **(1512)** by Application Programming Interface (API) **(1518)** through authentication process**.** Authentication **(1514)** includes entering valid userid and password credentials along with the one-time password (OTP) generated during the login. The MRI images are deidentified **(1508)** as per HIPPA **(1510)** guidelines at the time it was accessed from PACS. As soon as it enters the application, it passes through the models in sequential manner and predicts the results. The results **(1520)** are sent back to the PACS or VNA after re-identification **(1522).** The saved imaging results are obtained at any time from the PACS in DICOM format **(1524)** and the report is generated as a document **(1526)** and are assessed by neuroradiologists and oncologists. In the present disclosure, the web-based GUI application has excellent medical image visualization and several tools for simple computation like distance, angle, area, volume of the selected ROI. Integration of the application in the healthcare center is seamless **(1528)**. The services can be provided on premise or on cloud and can be accessible on mobile or desktop or laptop **(1530)**. The complete deployment workflow is shown in (**FIG. 15).**

[098] 11. IMPORTANT ATTRIBUTES OF THE DISCLOSED EMBODIEMNT

[099] This disclosure differs from the present technology by having higher AUC that is 99% and sensitivities greater than 90% for segmenting distinct subregions of the tumor.

[100] The present technologies perform automatic anatomical brain parcellation on MRI image as per requirement from the available brain atlas.

[101] In current clinical practice there is no provision for visualizing segmented tumor along with fiber tracts. The present disclosure combines 2D or 3D brain MRI image with the fiber tracts and tumor simultaneously in axial, sagittal and coronal planes and serves as pre-operative and intra-operative guidance for tumor surgery. It is far more advantageous than visualizing tumor or fiber tracts alone. It provides a clear assessment of any overlap between the fiber tract and tumor. Based on that the complete surgical planning is changed. During the surgery neurosurgeon minimizes the damage to the eloquent brain regions by protecting the important fiber tracts. This application can also be fed to neuronavigator for intra-operative surgical guidance.

[102] Present disclosure also provides information about genetic biomarkers that are the IDH subtypes non-invasively which otherwise difficult determine by non-invasive procedure. Correct identification of IDH subtype is important to start the preventive measures.

[103] Currently, Icometrix and brainomix from USA and Brainscan from Poland are the companies which provide solutions for brain abnormalities using AI. In India BrainSightAI is working in the neurological space.

[104] The major differentiator in our product from the available products are combined visualisation of segmented tumor subregions and the white matter fiber bundles on MRI images. Another important differentiator is non-invasive classification of gliomas into IDH subtypes.

[105] 12. HARDWARE

[106] **FIG. 16** is a block diagram illustrating the details of a digital processing system **(1600)** in which various aspects of the present disclosure are operative by

execution of appropriate execution modules, firmware, or hardware components.

[107] Digital processing system **(1600)** may correspond to each of user system: local system or remote server **(1612)**. Digital processing system may contain random access memory (RAM) **(1604),** one or more processors (such as a central processing unit (CPU) **(1606)**), secondary memory **(1602a, 1602b, 1602c),** central processing unit (CPU) **(1606)**, graphics controller (GPU) **(1608),** input /output interface **(1610),** network interfaces like (WLAN) **(1616).**

[108] CPU **(1606)** executes instructions stored in RAM **(1604)** to provide several features of the present disclosure. CPU **(1606)** may contain multiple processing units, with each processing unit potentially being designed for a specific task.

[109] Alternatively, CPU **(1606)** may contain only a single general purpose processing unit. RAM **(1604)** may receive instructions from secondary/system memory **(1602a, 1602b, 1602c).**

[110] Graphics controller (GPU) **(1608)** accelerate parallel processing task based on data/instructions received from input **(1618)**. Primary display unit contains a display screen **(1614)** (e.g., monitor, touchscreen, desktop, smartphone) to display the images defined by the display signals. Input interfaces **(1618)** may correspond to a keyboard, a pointing device (e.g., touch-pad, mouse), a touchscreen, etc. which enable the various inputs to be provided. Network interface **(1616)** provides connectivity to a network (e.g., using Internet Protocol), and may be used to communicate with other connected systems such as desktop **(1618)**, smart phone **(1620)** or laptop **(1622)**. Network interface **(1616)** may provide such connectivity over a wire (in the case of TCP/IP based communication) or wirelessly (in the case of WIFI, Bluetooth based communication).

[111] Secondary memory may contain hard drive (mass storage) **(1602a),** flash memory **(1602b),** and removable storage drive **(1602c).** Secondary memory may store the data (e.g., the specific requests sent, the responses received, etc.) and executable modules, which enable the digital processing system **(1600)** to provide several features in accordance with the present disclosure.

[112] Some or all of the data and instructions may be provided on a removable storage unit (SD card) **(1602c),** and the data and instructions may be read and

provided by removable storage drive **(1602c)** to CPU **(1606).** Floppy drive, magnetic tape drive, CD-ROM drive, DVD Drive, Flash memory, removable memory chip (PCMCIA Card, EPROM) are other examples of such removable storage drive. **(1602b, 1602c).**

[113] Removable storage unit **(1602c)** may be implemented using storage format compatible with removable storage drive such that removable storage drive **(1602c)** can read the data and instructions. Thus, removable storage unit **(1602c)** includes a computer readable storage medium having stored therein executable modules and/or data. However, the computer (or machine, in general) readable storage medium can be in other forms (e.g., non-removable, random access, etc.). CPU **(1606)** and GPU **(1608)** may retrieve the executable modules and execute them to provide various features of the present disclosure described above.

[114] 13. USES, APPLICATIONS AND BENEFITS OF THE DISCLOSED EMBODIEMNT

[115] The application is used for targeting glioma assessment. The key advantage is that it detects, performs tumor subregion segmentation, quantitative volumetric analysis, brain parcellation, tractography map generation and classification of gliomas into IDH subtypes non-invasively and efficiently.

[116] 14. BEST MODE TO PRACTICE

[117] The best mode to practice the disclosure is via B2B mode where hospitals/diagnostic centers are approached to use the application for tumor assessment and surgical planning of brain tumor.

[118] Merely for illustration, only representative number/type of graph, chart, block, and sub-block diagrams were shown. Many environments often contain many more block and sub-block diagrams or systems and sub-systems, both in number and type, depending on the purpose for which the environment is designed.

[119] While specific embodiments of the disclosed embodiments have been shown and described in detail to illustrate the inventive principles, it will be understood that the disclosed embodiments may be embodied otherwise without departing from such principles.

[120] Reference throughout this specification to “one embodiment”, “an

embodiment", or similar language means that a particular feature, structure, or characteristic described in connection with the embodiment is included in at least one embodiment. Thus, appearances of the phrases "in one embodiment", "in an embodiment" and similar language throughout this specification may, but do not necessarily, all refer to the same embodiment.

[121] It should be understood that the figures and/or screen shots illustrated in the attachments highlighting the functionality and advantages of the disclosed embodiments are presented for example purposes only. The disclosed embodiments are sufficiently flexible and configurable, such that it may be utilized in ways other than that shown in the accompanying figures.

[122] It should be understood that the examples and embodiments described herein are for illustrative purposes only and that various modifications or changes in light thereof will be suggested to persons skilled in the art and are to be included within the spirit and purview of this application and scope of the appended claims. All publications, patents, and patent applications cited herein are hereby incorporated by reference in their entirety for all purposes.

I/We Claim,

1. A method (FIG. 2) for gliomas classification, the method comprising:

receiving (202) a magnetic resonance imaging (MRI) image of a gliomas;

pre-processing (102, 208) the MRI image to obtain a processed MRI image (120) of the gliomas;

identifying (210) subregion segmentations of the gliomas in the processed MRI image, wherein each segmented subregion is one of peritumoral edema, enhancing tumor, non-enhancing tumor, or necrotic tumor (212);

determining (220) a classification of the gliomas based on the subregion segmentations of the gliomas, wherein the classification comprises isocitrate dehydrogenase (IDH) subtypes including glioblastoma, astrocytoma and oligodendroglioma (222); and

providing a visualization graphical user interface (GUI) for subregion segmentation of the gliomas and its classification into IDH subtypes.

2. The method of claim 1, wherein the MRI images are multiparametric comprising of T1-weighted (T1w), T2-weighted (T2w), post-contrast-T1 weighted (T1ce) and fluid attenuated inversion recovery (FLAIR), and diffusion weighted imaging (DWI),

wherein the MRI image is in Digital Imaging and Communications in Medicine (DICOM) format.

3. The method of claim 1, wherein the pre-processing (102, 208) comprises one or more of deidentification (104), conversion of the MRI image to Neuroimaging Informatics Technology Initiative (NIfTI) format (106), motion correction (108), BIAS correction (110), noise reduction (112), registration and resampling of the 3D volume of the MRI images (114), skull stripping (116) and normalization (118).

4. The method of claim 1, comprising:

training a segmentation Artificial Intelligence (AI) module (210) using a deep learning (DL) technique to correlate various portions of MRI images to subregion segmentations of gliomas,

wherein the identifying comprises providing the processed MRI image as input to the segmentation AI module to obtain as output segmented subregions of the gliomas in the processed MRI image.

5. The method of claim 1, comprising:

training a classification AI module (220) using a ML/DL technique to correlate features of the subregion segmentations of gliomas to classifications of gliomas,

wherein the determining comprises:

extracting (216) a set of features from the subregions of the gliomas, wherein the features include Visually Accessible Rembrandt Images (VARARI) features, radiomic features and clinical information;

selecting (218) a subset of significant features from the set of features, wherein the feature selection eliminates redundant features; and

providing the subset of significant features as input to the classification AI module to obtain the classification of the gliomas as output.

6. The method of claim 1, comprising deducing (214) volumetric quantifications for each segmented subregion of the gliomas.

7. The method of claim 1, comprising generating (402) a report including one or more of volume of the segmented subregions (404), differentiation between peritumoral edema and tumor core (406), location of the gliomas (408), identification of the fiber tracts present in close contact with the gliomas (410), textural features of the gliomas (412) and IDH subtypes of the gliomas (416).

8. A neuroimaging analytics and AI-driven system for gliomas classification (FIG. 3), the system comprising:

a pre-processing (306) module configured to receive a magnetic resonance imaging (MRI) image of a gliomas and to pre-process the MRI image to obtain a processed MRI image (120) of the gliomas;

a segmentation Artificial Intelligence (AI) module (210, 316) configured to identify subregion segmentations of the gliomas in the processed MRI image, wherein each segmented subregion is one of peritumoral edema, enhancing tumor, non-enhancing tumor, or necrotic tumor (212);

a classification AI module (220, 318) configured to determine a classification of the gliomas based on the features selected from subregions of the gliomas, wherein the classification comprises isocitrate dehydrogenase (IDH) subtypes glioblastoma, astrocytoma and oligodendroglioma (222); and

a brain parcellation module (310) configured to perform parcellation based on predefined atlas; and

a tractography map (314) of the brain generated from dMRI to visualize fiber tracts adjacent to the tumor;

and obtaining textural feature (312) of the tumor for reporting; and

a visualization module configured to provide a visualization (320) of the subregion segmentations of the gliomas and the classification.

9. The neuroimaging analytics and AI-driven system of claim 8, wherein the segmentation AI module (210) is trained using a ML/DL technique to correlate various portions of MRI images to the subregions of gliomas,
wherein the segmentation AI module is configured to receive the processed MRI image as input and provide as output segmented subregions of the gliomas in the processed MRI image.

10. The neuroimaging analytics and AI-driven system of claim 8, wherein the classification AI module (220) is trained using a ML/DL technique to correlate features of the segmented subregions of gliomas to classifications of gliomas,
wherein the system is configured to:

extract (216) a set of features from the segmented subregions of the gliomas, wherein the features include Visually Accessible Rembrandt Images (VARARI) features and clinical information;

select (218) a subset of significant features from the set of features, wherein the selecting also eliminates redundant features; and

provide the subset of significant features as input to the classification AI module to obtain an output the classification of the gliomas.

Dated this 29th day of March, 2024

(LIPIKA SAHOO)

Registration Number: IN/PA-2467

Agent for Applicant

This document is signed with the digital signature of Patent Agent for the Applicant LIPIKA SAHOO (IN/PA-2467)

ABSTRACT

NEUROIMAGING ANALYTICS AND AI- DRIVEN SYSTEM FOR GLIOMAS CLASSIFICATION USING MULTIPARAMETRIC MAGNETIC RESONANCE IMAGING

The present disclosure highlights the clinical assessment of adult diffuse gliomas. Multiparametric MRI images such as structural MRI and diffusion MRI are used in the establishment of this disclosure. Structural MRIs are used to identify the peritumoral edema, tumor core and enhancing tumor, its location, volumetric information, textural pattern of the tumor. Further brain parcellation is performed to understand anatomical organization of the brain with respect to the tumor location. In addition, tractography map is generated from the diffusion MRI and is used to visualize the white matter fiber tracts and its proximity to the tumor as the surgical guidance for pre-operative and intra-operative neurosurgery. Combined visualization of tumor and tractography in 3D space minimizes the damage to the eloquent brain during surgery. The disclosure assigns IDH subtypes to the adult diffuse gliomas non-invasively. These applications are integrated into the web-based GUI for visualization and clinical assessment of the gliomas.